Catalysis Communications 9 (2008) 1886–1890

Contents lists available at ScienceDirect

Catalysis Communications

journal homepage: www.elsevier.com/locate/catcom

Hydroxylation of benzene to phenol on Fe/TiO_2 catalysts loaded with different types of second metal

Garun Tanarungsun [a], Worapon Kiatkittipong [b], Piyasan Praserthdam [a], Hiroshi Yamada [c], Tomohiko Tagawa [c], Suttichai Assabumrungrat [a,*]

[a] Center of Excellence in Catalysis and Catalytic Reaction Engineering, Department of Chemical Engineering, Faculty of Engineering, Chulalongkorn University, Bangkok 10330, Thailand
[b] Department of Chemical Engineering, Faculty of Engineering and Industrial Technology, Silpakorn University, Nakhon Pathom 73000, Thailand
[c] Department of Chemical Engineering, Nagoya University, Chikusa, Nagoya 464-8603, Japan

ARTICLE INFO

Article history:
Received 26 October 2007
Received in revised form 23 February 2008
Accepted 4 March 2008
Available online 18 March 2008

Keywords:
Hydroxylation
Phenol production
Hydrogen peroxide
Metal oxide
TiO_2

ABSTRACT

This paper investigated the liquid phase hydroxylation of benzene to phenol with hydrogen peroxide over Fe/TiO_2-based catalysts. Various types of second metal (i.e., Ni, Co, Pd and Pt) were loaded together with Fe on the TiO_2 support and the catalytic performance of the obtained catalysts was compared. It was found that the presence of the second metal can improve the phenol production of the typical Fe/TiO_2 catalyst. The yield of phenol follows the order: Pt > Pd >> Co ≈ Ni. Various techniques (NH_3-TPD, XRD, BET surface area, SEM-EDX and XRF) were employed to characterize the Fe/TiO_2, $FePt/TiO_2$ and $FePd/TiO_2$ catalysts. The acid property of the catalyst was found to be influenced by the addition of the second metal. Finally the effects of some operating variables (reaction time, H_2O_2/benzene ratio and amount of ascorbic acid) on the catalytic performance were investigated.

1. Introduction

Phenol is an important intermediate for the synthesis of petrochemicals, agrochemicals and plastics. Nowadays approximately 95% of phenol production was produced by cumene process consisting of three main reaction steps (alkylation of benzene with propylene to cumene, oxidation of cumene to cumene hydroperoxide and decomposition to phenol and acetone). The direct oxidation of benzene to phenol, a one-step reaction, is an attractive process under investigation nowadays due to the potential simplification of the production process. Various oxidants, such as nitrous oxide [1,2], hydrogen peroxide [3–8], oxygen [9,10], or mixture of oxygen and hydrogen [11,12] have been employed for the direct oxidation of benzene to phenol. Among them, the hydroxylation of benzene to phenol with hydrogen peroxide was probably the most effective route to achieve high conversion and yield [13]. Hydrogen peroxide, besides molecular oxygen, is the most attractive oxidant because it is of comparatively low cost and gives only water as a byproduct [13].

Many transition metal catalysts have been employed for catalyzing the hydroxylation of benzene to phenol but so far no appreciable success has been achieved. It has been reported that Fe, Cu and V catalysts are effective for the oxidation of benzene by O_2 or H_2O_2 with ascorbic acid as a reducing agent [14–20]. Liu et al. [21] reported that the performance of the substituted transition metal in the polyoxometalate compounds (TMSP) on the benzene conversion followed the order: Cu > V > Fe. The reaction mechanisms over Fe, Cu and V catalysts were proposed to follow Fenton reaction.

The Fenton reaction has been well-known as the reaction for oxidation of aromatic compounds. Many researchers studied the oxidation reaction with Fe due to its low cost. Although high conversion can be obtained, the selectivity was rather low because the reaction is frequently accompanied by the formation of byproducts such as biphenyl and further oxidation compounds of phenol [13]. To improve catalytic performance of a catalyst, it is customary to add a second metal on the catalyst to alter its catalytic properties. Noble metals, such as Pt, Pd, and Au, have been applied to improve the activity of transition metal oxide catalysts. Pd and Pt are well-known for the hydrogenation reaction [7]. Some researchers have employed Pt and Pd as a co-catalyst to improve the activity of a based metal oxide catalyst. Because Pt and Pd changed the oxidation state of metal oxide catalyst and converted O_2 and H_2 to H_2O_2, the activity for the oxidation reaction is therefore improved [11].

* Corresponding author. Tel.: +662 2186868; fax: +662 2186877.
E-mail address: Suttichai.A@chula.ac.th (S. Assabumrungrat).

1566-7367/$ - see front matter © 2008 Elsevier B.V. All rights reserved.
doi:10.1016/j.catcom.2008.03.008

In this study, we attempted to improve the catalytic properties of the Fe/TiO_2 catalyst for the liquid phase hydroxylation of benzene to phenol with hydrogen peroxide at room temperature. Fe is selected as the main catalyst due to its low cost. Various types of second metals (i.e., Ni, Co, Pd and Pt) were loaded together with Fe on the catalysts for selecting suitable metals for this reaction system. Different characterization techniques were performed to understand the role of the second metal. Finally, the effects of some operating variables such as reaction time, ratio of H_2O_2: benzene and amount of reducing agent on the phenol yield were investigated.

2. Experimental

2.1. Catalyst preparation

Catalysts were prepared by impregnating TiO_2 (JRC-TIO1) support powder in a solution of mixture of metal precursors at 353 K followed by evaporation and drying for overnight. The metal precursors were palladium (II) nitrate, platinum (II) diamine dichloride, cobolt (II) nitrate, nickel (II) nitrate hexahydrate and iron (III) acetylacetonate. The obtained catalysts were then calcined in a furnace whose temperature was increased from room temperature to 773 K at a heating rate of 10 K/min and held for 5 h to remove the organic residues. After calcinations, the catalysts were stored in a dessicator.

2.2. Characterization

XRD patterns of the TiO_2 support and metal supported catalysts were obtained by using X-ray diffractrometer, D 5000 (Siemens AG) using Cu Kα radiation equipped with Ni filter with a range of detection of 2θ 20–80 and a resolution of 0.04.

BET surface area and porosity of the catalysts were measured by Micromeritics ASAP 2020. A sample of 0.3 g was degassed at 573 K for 3 h and the amount of N_2 adsorption was recorded.

X-ray fluorescence analysis (XRF) was performed to determine composition in the bulk of catalysts. The analysis was performed using Siemens SRS3400.

Ammonia-temperature programmed desorption (NH_3-TPD) was carried out using a Micromeritics 2000 TPD/TPR instrument. A catalyst sample (0.1 g) was treated in a helium flow for 1 h at 523 K for removing water and degassing of the catalyst. Then it was saturated in a flow of 15% NH_3/He mixture after cooling to room temperature. After purging with helium at room temperature for 1 h to remove weakly physisorbed NH_3, the sample was heated to 1023 K at a rate of 10 K/min in a helium flow (30 cm^3/min).

Scanning electron microscopy (SEM) and Energy dispersive X-ray spectroscopy (EDX) techniques were used to determine the catalyst granule morphology and elemental distribution of the catalyst particles using JEOL JSM-5800LV scanning electron microscope. The SEM was operated in the back scattering electron (BSE) mode at 20 kV. EDX was performed to determine the elemental concentration distribution on the catalyst granules using Link Isis Series 300 software.

2.3. Experimental setup and product analysis

The oxidation of benzene by H_2O_2 was carried out in a 125 cm^3 round flat bottomed flask at 303 K and 1 atm with a high speed stirrer. The reaction system consisted of two liquid phases: an organic phase containing a substrate (benzene) and solvent (acetonitrile), and an aqueous phase containing 30 wt% H_2O_2 and some acetonitrile.

In a typical experiment, 0.2 g of catalyst was added in a liquid mixture containing 40 cm^3 of acetonitrile, 30 cm^3 (0.32 mol) of H_2O_2 and 11 cm^3 (0.16 mol) of benzene.

The feed and products were analyzed by a gas chromatograph (GC 9A, Shimazu Corp.) with a packed column of GP 10% SP-2100. The injection temperature of 523 K, detector temperature of 523 K, initial column temperature of 383 K, final column temperature of 443 K and temperature programmed rate of 10 K/min were employed. The products were also analyzed by GC–MS especially for some product species which cannot be detected by the FID detector.

The metal loadings of catalyst were calculated as the weight of metal divided by the weight of metal added TiO_2.

The terms of reaction performance were defined as follows:

$$\text{Conversion of benzene} = \frac{\text{mole of benzene reacted}}{\text{initial mole of benzene}}$$

$$\text{Selectivity of phenol} = \frac{\text{mole of phenol produced}}{\text{mole of benzene reacted}}$$

$$\text{Yield of phenol} = \frac{\text{mole of phenol produced}}{\text{initial mole of benzene}}$$

3. Results and discussion

3.1. Catalyst screening and catalyst characterization

Table 1 shows the catalytic performance in the hydroxylation of benzene on several TiO_2-supported binary metal oxide catalysts (Fe/TiO_2, FeNi/TiO_2, FeCo/TiO_2, FePd/TiO_2 and FePt/TiO_2), together with TiO_2 without metal oxides. Note that the values in the blanket represent the weight percentages of the metals. The BET surface area and pore volume were slightly decreased by adding Fe and second metal in the support.

For the Ni and Co co-catalysts, slightly higher yields than that of the single iron oxide catalyst were obtained. The results may confirm the catalytic behavior of Ni and Co metals reported earlier by Dubey et al. [22–24] that from the selection of different metals, Ni and Co as bivalent cations on ternary hydrotalcite catalyst showed high activity for hydroxylation of phenol. It may be concluded that catalysts containing Ni and Co were not suitable for hydroxylation of benzene to phenol but suitable for hydroxylation of phenol.

On the contrary, significant improvement of phenol yield can be achieved by doping small amount of Pd or Pt. The activities of the co-catalysts were ordered as: Pt > Pd >> Co ≈ Ni. It should be noted that, all of the mentioned metals were reported to offer the same degree for decomposition reaction of hydrogen peroxide. Rufus et al. [25] investigated the in situ deposition of various metals on CdS during the photocatalytic decomposition of aqueous sulfide. The order of reactivity was: Rh > Pt > Pd > Ru = Ir > Co ≈ Ni. Therefore, the Pt and Pd were selected for further characterization and reaction study.

Table 1
Summary of catalytic performance and some physical properties of different catalysts

Catalyst	Conversion (%)	Selectivity (%)	Yield (%)	BET (m^2/g)	Pore volume (cm^3/g)
TiO_2	N.D.	N.D.	0.19	74.5	0.26
Fe/TiO_2 (5%)	N.D.	N.D.	1.36	71.0	0.26
FeNi/TiO_2 (5%,1%)	2.2	65	1.43	70.2	0.24
FeNi/TiO_2 (5%,2.5%)	3.0	56	1.68	69.3	0.26
FeCo/TiO_2 (5%,2.5%)	3.3	58	1.91	67.5	0.24
FePd/TiO_2 (5%,1%)	6.7	80	5.36	65.4	0.23
FePt/TiO_2 (5%,1%)	6.5	91	5.92	65.1	0.22

N.D. = Not determined. (Benzene = 11 cm^3;%Fe (III) loading = 5 wt%; catalyst weight = 0.2 g; H_2O_2/benzene mole ratio = 2; acetronitrile solvent 40 cm^3; ascorbic acid = 0.5 g; temperature = 303 K; pressure = 1 atm; reaction time = 4 h).

The chemical composition of the catalyst on the surface and bulk composition of Fe/TiO_2, $FePd/TiO_2$ and $FePt/TiO_2$ were determined by SEM-EDX and XRF, respectively. The comparable results obtained from SEM-EDX and XRF suggest that the metal species were deposited at least on the surface of the support. However, it should be noted that the amounts of iron, platinum, palladium of the catalysts are not quite in good agreement with the applied metal loading (not shown).

The XRD patterns of the support and the catalysts were determined; however, there are no significant changes in XRD spectra between Fe supported on TiO_2 and binary metal oxide supported on TiO_2. It is probably because the amount of Pt or Pd in the catalyst was low.

The results of NH_3-TPD showed that the second metal loading of Pt or Pd influenced the acid property of the catalyst. As shown in Fig. 1, only one peak at $T \approx 443$ K was observed for Fe/TiO_2. However, by loading Pt or Pd, a peak at a lower temperature ($T \approx 373$ K) and an additional peak at higher temperature (623–723 K) were observed. The presence of the second metal obviously altered the acid property of the catalysts. As it was reported that the acidic condition was necessary for the system of ferrous and ferric ions in the liquid phase hydroxylation of benzene to phenol [3], it is likely that the use of the second metal helped increase the activity of the Fenton reaction of iron oxide in the catalyst by altering the acid property of the catalyst. The strong acid site (at high temperature) was more pronounced in the case of Pt. This may be the reason why Pt gives higher phenol yield than that of Pd. It was reported that Pt might promote the reducibility of iron oxide (FeO_x) and probably could act together with reduced FeO_x species in a concert mechanism in benzene oxidation. Pt is well-known for the hydrogenation reaction [7] while iron oxide is well-known for oxidation. Therefore the interaction between iron or Pt and H_2O_2 would be expected. H_2O_2 was decomposed to hydroxyl radical on the precious metal, i.e., Pt [12].

3.2. Effect of reaction time

Fig. 2 shows the influence of reaction time on the phenol yield. The reaction occurs similar to Fenton chemistry, through the participation of hydroxyl radical in activating benzene toward the formation of phenol. Increasing the reaction time directly increased the benzene conversion. It should be noted that the catalyst deactivation was not checked in this study. The obtained results indicated that after 4 h the phenol selectivity decreased as observed by the increase of byproducts in the system. In the H_2 and O_2 system, H_2O_2 was formed from both gases on the platinum and this H_2O_2 was decomposed to hydroxyl radical on the platinum. It is likely that the platinum and palladium could increase the amount of hydroxyl radical and form water due to the decomposition of H_2O_2.

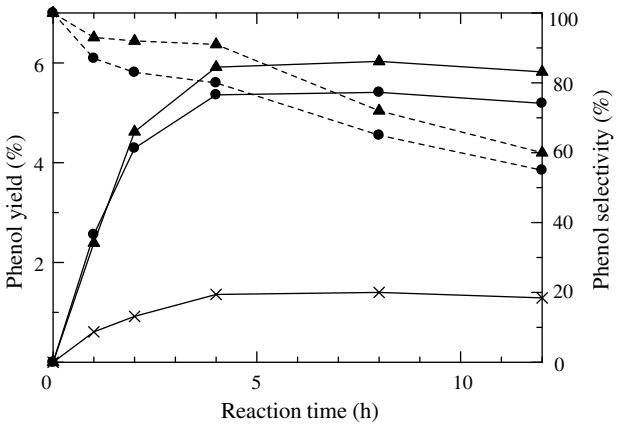

Fig. 2. Effect of reaction time on phenol yield (—) and selectivity (---) for different catalyst i.e., × Fe/TiO_2, ● $FePd/TiO_2$, ▲ $FePt/TiO_2$.

The mechanism of Fenton's method is widely accepted as follows [26]:

$$Fe^{2+} + H_2O_2 \rightarrow Fe^{3+} + OH^0 + OH^- \quad (1)$$

The hydroxyl radical reacts directly with benzene to produce cyclohexadienyl (CHD) radical, which subsequently undergoes an H^+ abstraction as follows:

$$OH^0 + \text{benzene} \rightarrow \text{CHD} \quad (2)$$

$$\text{CHD} + Fe^{3+} \rightarrow \text{phenol} + Fe^{2+} + H^+ \quad (3)$$

However, the CHD radical intermediate can react with H^+ and collapse to benzene as follows:

$$\text{CHD} + Fe^{2+} + H^+ \rightarrow \text{benzene} + Fe^{3+} + H_2O \quad (4)$$

3.3. Effect of the amount of H_2O_2 for the hydroxylation of benzene

The effect of the ratio of H_2O_2: benzene on yield of phenol was shown in Fig. 3. In the cases of Pt and Pd modified catalysts, phenol yield increased with increasing the ratio of H_2O_2 per benzene up to 2 and then decreased. It can be explained that further oxidation of phenol to hydroquinone, benzoquinone and other products can be

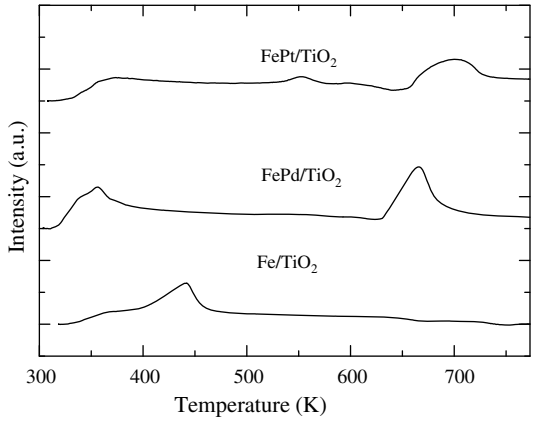

Fig. 1. NH_3-TPD results of different catalysts.

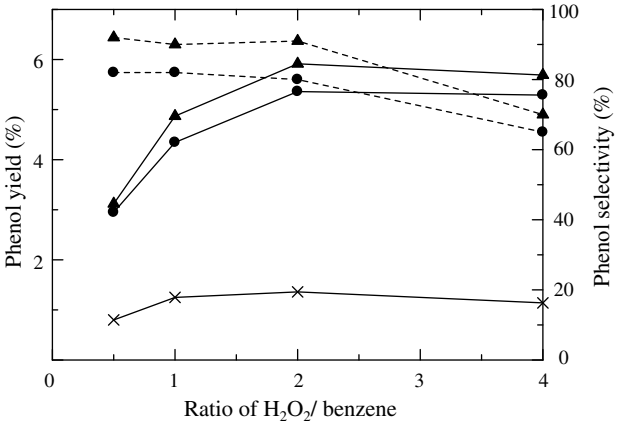

Fig. 3. Effect of H_2O_2/benzene ratio on phenol yield (—) and selectivity (---) for different catalyst i.e., × Fe/TiO_2, ● $FePd/TiO_2$, ▲ $FePt/TiO_2$ (4 h reaction time).

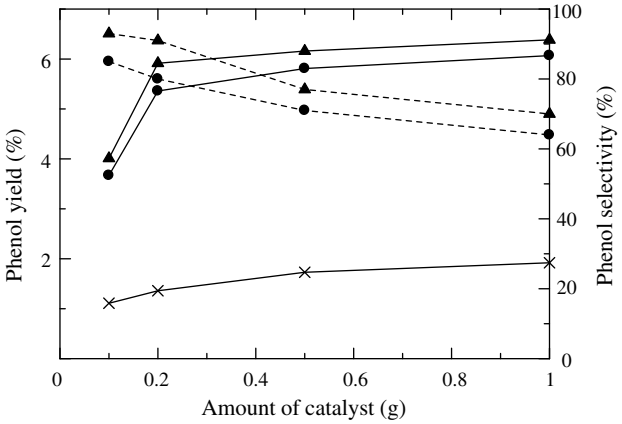

Fig. 4. Effect of amount of catalyst on phenol yield (—) and selectivity (---) for different catalyst i.e., × Fe/TiO_2, ● $FePd/TiO_2$, ▲ $FePt/TiO_2$ (4 h reaction time).

occurred with the presence of excessive amount of H_2O_2 oxidant. At a high oxidant concentration, it was difficult to control the selective oxidation to produced phenol. The benzene conversion was increased by the high concentration of oxidant but it decreased the phenol selectivity.

3.4. Effect of the amount of catalyst

The influence of the amount of catalyst on the yield of phenol over binary metal oxide supported on TiO_2 catalyst at room temperature is illustrated in Fig. 4. The yield of phenol increased with increasing the amount of catalyst.

The catalyst concentration has the effect on the decomposition of hydrogen peroxide and the amount of hydroxyl radical for the reaction. Increasing the amount of catalyst increased the conversion and yield but decreased phenol selectivity. The phenol was easy to oxidize to other products (hydroquinone, benzoquinone and cresol). Therefore, phenol yield did not increase at high concentration of catalyst.

3.5. Effect of the amount of ascorbic acid

The dependence of the phenol yield on the amount of ascorbic acid was investigated at room temperature as shown in Fig. 5. The yield of phenol increased with increasing the amount of ascorbic acid up to 1 g. Further increase in the amount of ascorbic acid insignificantly affected the phenol yield. The use of excessive amount of ascorbic acid, which functioned as a reducing agent, led to the reductive decomposition of hydrogen peroxide. In this case, increasing the amount of ascorbic acid increased the benzene conversion and decreased the selectivity of phenol.

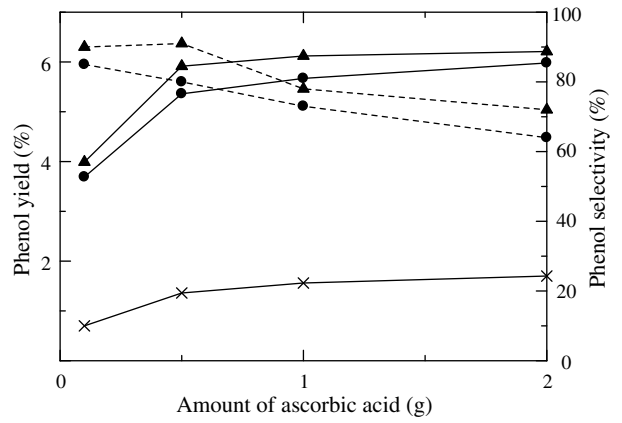

Fig. 5. Effect of amount of ascorbic acid on phenol yield (—) and selectivity (---) for different catalyst i.e., × Fe/TiO_2, ● $FePd/TiO_2$, ▲ $FePt/TiO_2$ (4 h reaction time).

The ascorbic acid is well-known as a good reducing agent. It changes the state of metal catalyst from Fe (III) to Fe (II) [4–6].

$$2Fe^{3+} + \text{ascorbic acid} + 0.5O_2 \rightarrow 2Fe^{2+} + \text{dehydroascorbic acid} + H_2O \quad (5)$$

$$2Fe^{2+} + O_2 + 2H^+ \rightarrow 2Fe^{3+} + H_2O_2 \quad (6)$$

$$Fe^{3+} + H_2O_2 + H^+ \rightarrow Fe^{2+} + OH^0 + H_2O \quad (7)$$

As the active species (Fe^{2+}) was regenerated by ascorbic acid, the effect of ascorbic acid was similar to the case of increasing the amount of catalyst.

4. Conclusion

The liquid phase hydroxylation of benzene to phenol with hydrogen peroxide catalyzed by Fe-containing binary metal oxide catalysts supported on TiO_2 was investigated. The second metal can improve the phenol production of the typical Fe/TiO_2 catalyst in the order of Pt > Pd >> Co ≈ Ni. Doping with 1 wt% Pt or Pd obviously improved phenol yield. The presence of the Pt or Pd obviously altered the acid property of the catalyst which is favorable for the Fenton reaction. At too long reaction time or too large amount of H_2O_2 oxidant or catalyst or ascorbic acid, byproducts (benzoquinone, hydroquinone and cresol) could be produced. The optimum condition for the system is 4 h of reaction time with the ratio of 2 moles of H_2O_2, 1.25 g of catalyst and 6.25 g of ascorbic acid per mole of benzene.

Acknowledgements

Financial support from the Thailand Research Fund and Commission on Higher Education is gratefully acknowledged.

References

[1] H. Yamanaka, R. Hamada, H. Nibuta, S. Nishiyama, S. Tsuruya, J. Mol. Catal. A: Chem. 178 (2002) 89.
[2] J.L. Motz, H. Heinichen, W.F. Holderich, J. Mol. Catal. A: Chem. 136 (1998) 175.
[3] Y.J. Seo, Y. Mukai, T. Tagawa, S. Goto, J. Mol. Catal. A: Chem. 120 (1997) 49.
[4] G. Tanarungsun, W. Kiatkittipong, S. Assabumrungrat, H. Yamada, T. Tagawa, P. Prasertdam, J. Chem. Eng. Jpn. 40 (2007) 415.
[5] G. Tanarungsun, W. Kiatkittipong, S. Assabumrungrat, H. Yamada, T. Tagawa, P. Prasertdam, J. Ind. Eng. Chem. 13 (2007) 444.
[6] G. Tanarungsun, W. Kiatkittipong, S. Assabumrungrat, H. Yamada, T. Tagawa, P. Prasertdam, J. Ind. Eng. Chem. 13 (2007) 870.
[7] X. Gao, J. Xu, Appl. Clay Sci. 33 (2006) 1.
[8] Y.K. Masumoto, R. Hamada, K. Yokota, S. Nishiyama, S. Tsuruya, J. Mol. Catal. A: Chem. 184 (2002) 215.
[9] H. Kanzaki, T. Kitamura, R. Hamada, S. Nishiyama, S. Tsuruya, J. Mol. Catal. A: Chem. 208 (2004) 203.
[10] T. Ohtani, S. Nishiyama, S. Tsuruya, M. Masai, J. Catal. 155 (1995) 158.
[11] N.I. Kuznetsova, L.I. Kuznetsova, V.A. Likholobov, G.P. Pez, Catal. Today 99 (2005) 193.
[12] T. Miyake, M. Hamada, Y. Sasaki, M. Oguri, Appl. Catal. A: Gen. 131 (1995) 33.
[13] H.H. Monfared, Z. Amouei, J. Mol. Catal. A: Chem. 217 (2004) 161.
[14] K. Fujushima, A. Fukuoka, A. Yamagishi, S. Inagaki, Y. Fukushima, M. Ichikawa, J. Mol. Catal A: Chem. 166 (2000) 211.
[15] C.W. Lee, W.J. Lee, Y.K. Park, S.E. Park, Catal. Today 61 (2000) 137.
[16] K. Teramura, T. Tanaka, T. Hosokawa, T. Ohuchi, M. Kani, T. Funabiki, Catal. Today 96 (2004) 205.
[17] K. Lemke, H. Eric, U. Lohse, H. Berndt, K. Jahnisch, Appl. Catal. A: Gen. 243 (2003) 41.
[18] R.S.G. Ferreira, P.G.P. de Oliveira, F.B. Noronha, Appl. Catal. B: Environ. 50 (2004) 243.
[19] J. Zhang, Y. Tang, G. Li, C. Hu, Appl. Catal. A: Gen. 278 (2005) 251.
[20] V. Parvulescu, B.L. Su, Catal. Today 69 (2001) 315.

[21] Y. Liu, K. Murata, M. Inaba, Catal. Commun. 6 (2005) 679.
[22] A. Dubey, V. Rives, S. Kannan, J. Mol. Catal. A 181 (2002) 151.
[23] A. Dubey, V. Rives, S. Kannan, Phys. Chem. Chem. Phys. 3 (2001) 4826.
[24] A. Dubey, S. Kannan, S. Velu, K. Suzuki, Appl. Catal. A: Gen. 238 (2003) 319.
[25] I.B. Rufus, B. Viswanathan, V. Ramakrishnan, J.C. Kuriacose, J. Photochem. Photobiol. A: Chem. 91 (1995) 63.
[26] T. Miyahara, H. Kanzaki, R. Hamada, S. Kuroiwa, S. Nishiyama, S. Tsuruya, J. Mol. Catal. A: Chem. 176 (2001) 141.

Appendix 15

Journal of the Japan Petroleum Institute, **51**, (2), 114–117 (2008)

[Research Note]

Catalyst Regenerator for Partial Oxidation of Benzene in Reaction-extraction System

Hiroshi YAMADA[†1]*, Tomoaki MIZUNO[†1], Tomohiko TAGAWA[†1], Garun TANARUNGSUN[†2], Piyasan PRASERTHDAM[†2], and Suttichai ASSABUMRUNGRAT[†2]

[†1] Dept. of Chemical Engineering, Nagoya University, Chikusa-ku, Nagoya 464-8603, JAPAN
[†2] Center of Excellence in Catalysis and Catalytic Reaction Engineering, Dept. of Chemical Engineering, Chulalongkorn University, Bangkok 10330, THAILAND

(Received November 19, 2007)

The liquid-phase oxidation of benzene to phenol was investigated in the biphasic benzene-water system using VCl_3 and molecular oxygen as the catalyst and oxidant, respectively. Benzene was dissolved in the aqueous catalyst phase and reacted with oxygen to form phenol. Phenol was preferentially extracted into the benzene phase, thus suppressing the formation of over-oxidized byproducts. During the reaction, the catalyst was oxidized and deactivated. To regenerate the catalyst, a regenerator was installed into the system. Hydrogen was fed to the regenerator to reduce the deactivated catalyst, but no significant improvement of the system performance was observed without the presence of a second catalyst. Pd sheet in the regenerator allowed the system to run very stably, and the system was easy to shut down and start up.

Keywords
Benzene, Phenol, Partial oxidation, Bi-phase system, Reaction-extraction system

1. Introduction

Commercial production of phenol generally depends on the indirect-multistage cumene process which produces equimolar amounts of acetone as a byproduct. Therefore, methods for direct oxidation of benzene to phenol under mild conditions are desirable. Many catalysts such as Cu[1], V[2),3)], Pd[4),5)] and Pt[5)] have been investigated for direct oxidation with molecular oxygen. However, a few efforts have focused on the design of reactors or reaction systems for the direct oxidation of benzene. A stirring batch reactor was used in a bi-phase system[6)]. Benzene and hydrogen peroxide were separated by a membrane which allowed benzene to permeate across the membrane to the aqueous phase whereas phenol permeated back to the organic phase. The system had high selectivity for phenol, and minimized over-oxidation to form byproducts. Selectivity for phenol of 99.94% could be achieved with a hydrophobic porous polypropylene membrane. A palladium membrane reactor was used in a gas phase reaction[7)]. Hydrogen was activated during permeation across the membrane. The active hydrogen atoms reacted with oxygen molecules to form active species like O or OH radicals, which then attacked benzene to produce phenol. The yield of phenol was 20%. We previously proposed the liquid-phase oxidation of benzene to phenol in a biphasic benzene-water system[8)]. Catalyst deactivation was found to be a major problem in the process.

The present study improved the liquid-phase oxidation of benzene to phenol in the biphasic benzene-water system by incorporating a regenerator into the reactor-extractor system. **Figure 1** shows the concept of the proposed system consisting of a reactor, an extractor, and a regenerator. The reactor contains both benzene phase and aqueous phase. Benzene dissolved into the aqueous phase is oxidized to phenol which is then extracted into the benzene phase. Further oxidation of phenol does not take place in the benzene phase because the catalyst is selectively dissolved in the aqueous phase. However, further oxidation of phenol can occur in the aqueous phase. Therefore, phenol dissolved in the benzene phase is removed from the reactor by the extractor. Benzene phase is pumped by a circulation pump from the reactor to the extractor which contains aqueous NaOH solution, where phenol is extracted into the alkaline solution as phenoxide. Only benzene is returned to the reactor. The regenerator is used to regenerate the deactivated catalyst. The aqueous phase containing the catalyst is pumped from the reactor to the regenerator where hydrogen gas is used to reactivate the catalyst.

* To whom correspondence should be addressed.
* E-mail: yamada@nuce.nagoya-u.ac.jp

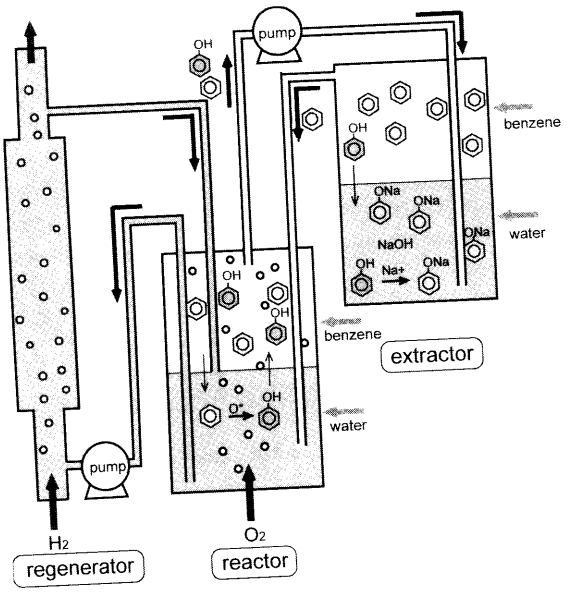

Fig. 1 Reactor System

2. Experimental

Figure 1 shows the all glass apparatus used in this study. Two jacketed stirred tank reactors were used as the reactor and the extractor and a bubble column reactor as the regenerator. Benzene (6.0×10^{-5} m^3) and water (1.0×10^{-4} m^3) were placed in the reactor and oxygen (2.5×10^{-5} m^3/min) was continuously introduced. VCl_3 catalyst was dissolved in the aqueous phase at a concentration of 10 mol/m^3-aq. Benzene (1.4×10^{-4} m^3) and aqueous NaOH solution (1.0×10^{-4} m^3 with a concentration of 1.2 mol/m^3-aq) were placed in the extractor. Benzene phase was circulated between the reactor and the extractor using a circulation pump. The flow rate was controlled at 3.5×10^{-5} m^3/min. The temperature of the reactor and the extractor was fixed at 313 K in all experiments. The regenerator containing the aqueous catalyst solution (1.0×10^{-4} m^3) was continuously fed with hydrogen (2.5×10^{-5} m^3/min). Another circulation pump was used to circulate the aqueous solution between the reactor and the regenerator. The flow rate was set at 3.7×10^{-5} m^3/min. The regenerator was operated at 313 or 333 K.

All chemicals used in this study were purchased from Wako Pure Chemical Industries, Ltd. No further purification was carried out. A small amount of sample was periodically analyzed with a gas chromatograph (GC-353B, GL Sciences, Inc.) equipped with a 25 m column (CP-Sil 8CB, J&W Scientific, Inc.) operated at 393 K. GC-MS (gas chromatograph-mass spectrometer, HP6890GC-HP5972A, Hewlett Packard Co., Ltd.) with a 60 m column (HP-INNOWAX, Hewlett Packard Co., Ltd.) was used to identify any byproduct.

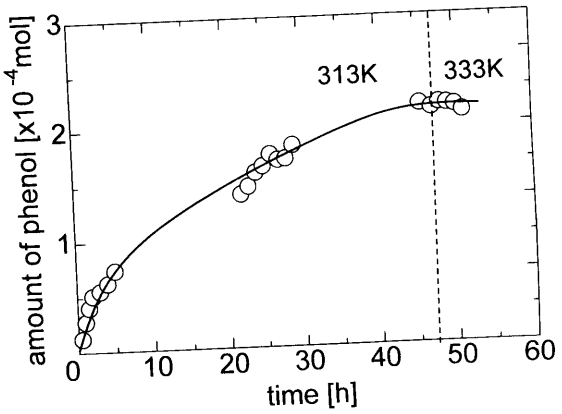

Fig. 2 Reaction Profile Using Regenerator without Reduction Catalyst

3. Results and Discussion

Hydroquinone, byproduct, was detected when the extractor was not used. However, no byproduct was detected after including the extractor into the system.

In this benzene and aqueous biphasic reaction system, the reaction occurs in the aqueous phase which contains the catalyst. The benzene dissolved in the aqueous phase was consumed by the reaction but it is supplied from benzene phase where far excess amount of benzene is charged as an extracting solvent. The benzene concentration depends only on the solubility of benzene in water. As excess benzene is charged into the reaction system, conversion based on charged benzene does not show the catalytic performance. Therefore, the time course of phenol formation is mainly discussed.

At first the regenerator was operated without reducing catalyst. The operation temperature was 313 K, the same temperature as those of the reactor and extractor. The reaction profile shown in **Fig. 2** indicated that after running the system for 45 h, the production of phenol apparently stopped due to catalyst deactivation. To promote regeneration of the catalyst by hydrogen, the temperature of the regenerator was increased to 333 K. However, no significant improvement was detected.

A new experiment was then carried out with reducing catalyst packed in the regenerator. To reduce the over-oxidized vanadium species with hydrogen, 30 g of 0.5 wt% Pd/Al_2O_3 (Sigma Aldrich, Inc.) was packed into the regenerator which was operated at 333 K. **Figure 3** clearly shows that the use of Pd/Al_2O_3 improved the performance of the reaction system, but phenol formation stopped within 50 h. The same amount of VCl_3 catalyst as used in the initial experiment was added to the system. The system then began to produce phenol again and continued until 190 h. The color of the catalyst (aqueous) phase changed during the reaction from the initial brownish green to pale blue after 1 h, which faded with time and finally became color-

Table 1 Investigation of Vanadium Adsorption

sample	initial conc. [ppm]	3 days after [ppm]	adsorption ratio [%]
V	10.33	10.33	0
V + Zr	10.33	8.75	15.3
V + Pd/Al_2O_3	10.33	0.023	99.8

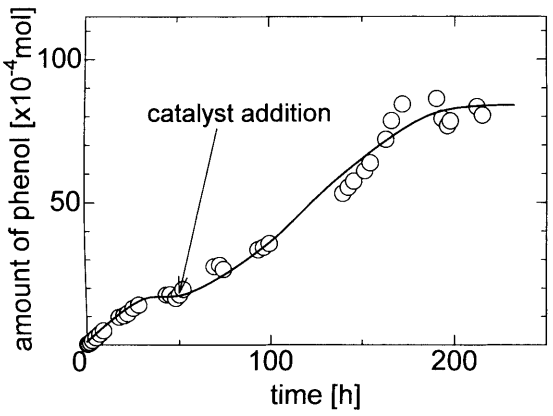

Fig. 3 Reaction Profiles Using Regenerator with Pd/Al_2O_3

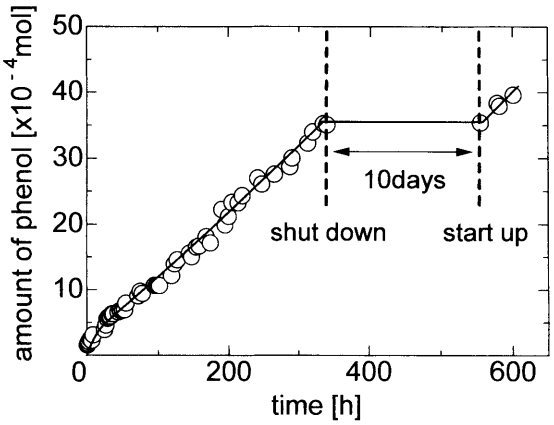

Fig. 4 Reaction Profiles Using Regenerator with Pd/sheet

less and transparent. Phenol formation rate decreased and became zero as the catalyst phase became colorless.

After new catalyst was added, the color cycle was repeated. V^{2+}, V^{3+}, V^{4+} and V^{5+} ions are colored purple, green, blue, and transparent, respectively. We used VCl_3 as a catalyst precursor, so the catalyst phase was dark green at first. The catalyst phase became pale blue showing V^{3+} was oxidized to blue V^{4+}. At this stage, the main vanadium species in the reactor was V^{4+}. This oxidation process activated molecular oxygen as in Fenton's method. There are two hypotheses for the declining performance of the system: oxidation of the catalyst from V^{4+} to V^{5+}, and adsorption of vanadium ion onto the Pd/Al_2O_3 catalyst in the regenerator. In both cases, the color of the catalyst phase eventually becomes transparent.

A set of experiments was carried out to investigate the adsorption of vanadium on the Pd/Al_2O_3 catalyst. VCl_3 0.063 g was dissolved into 30 cm^3 water. Pd/Al_2O_3 6.0 g was stood in the solution for 3 days at 333 K. As ZrO_2 balls were packed on top of the Pd/Al_2O_3 layer to fix the catalyst in the regenerator, adsorption of VCl_3 onto ZrO_2 balls (10 g) was also tested under the same conditions. **Table 1** summarizes the results. Concentrations were determined by ICP (inductively coupled plasma) atomic emission spectrometer. Pd/Al_2O_3 preferentially adsorbed vanadium ions whereas ZrO_2 balls slightly adsorbed vanadium ions. Therefore, the loss of the catalytic activity shown in **Fig. 3** was caused by adsorption of the vanadium species on the Pd/Al_2O_3 catalyst in the regenerator. Al_2O_3 is porous and has high surface area, so is likely to be a good medium for adsorbing metal ions. **Figure 3** also shows that added vanadium catalyst could produce much larger amounts of phenol than the initial vanadium charge, because the adsorption of initial vanadium retarded the adsorption rate of the added vanadium. This resulted in the prolonged apparent catalyst life of the added vanadium. A supported catalyst in the regenerator may not be a good choice unless a large excess of vanadium catalyst is involved in this system. Therefore, a palladium metal bulk catalyst was tested.

Bulk regeneration catalyst formed of palladium sheet (12.3 g, 100 × 100 × 0.1 mm, Nilaco Co.) was inserted in the regenerator. **Figure 4** shows that phenol could be produced in the system without deactivation for more than two weeks. Therefore, adsorption of active vanadium species onto the regeneration catalyst was avoided. The formation rate of phenol was smaller than that of Pd/Al_2O_3 as expected because of the difference in surface area between the Pd sheet and the supported Pd catalyst.

An experiment was continued to test the shut-down and start-up operation. To shut down the system, the temperature was decreased to room temperature and gaseous feed was stopped at 340 h. After 10 days, the system was started up again. As shown in **Fig. 4**, phenol was produced again and the formation rate of phenol was almost same as in the previous run. Therefore, the system was very stable, and easy to shut down and start up.

4. Conclusion

The combined reactor, extractor and regenerator system for the organic-aqueous liquid-phase oxidation of

benzene to phenol with gaseous oxygen under water soluble vanadium catalyst could reactivate the deactivated catalyst for continuous operation. Although Pd/Al_2O_3 catalyst could regenerate the catalyst, operation suffered from the adsorption of vanadium ion on the Al_2O_3 support. Use of palladium sheet in the regenerator allowed the system to run very stably, and allowed easy shut down and start up.

References

1) Miyahara, T., Kanzaki, H., Hamada, R., Kuroiwa, S., Nishiyama, S., Tsuruya, S., *J. Mol. Catal. A*, **176**, 141 (2001).
2) Masumoto, Y., Hamada, R., Yokota, K., Nishiyama, S., Tsuruya, S., *J. Mol. Catal. A*, **184**, 215 (2002).
3) Lemke, K., Ehrich, H., Lohse, U., Berndt, H., Jaehnisch, K., *Appl. Catal. A: General*, **243**, 41 (2003).
4) Burton, H. A., Kozhevnikov, I. V., *J. Mol. Catal. A*, **184**, 285 (2002).
5) Kuznetsova, N. I., Kuznetsova, L. I., Likholobov, V. A., Pez, G. P., *Catal. Today*, **99**, 193 (2005).
6) Molinari, R., Poerio, T., Argurio, P., *Catal. Today*, **118**, 52 (2006).
7) Itoh, N., Niwa, S., Mizukami, F., Inoue, T., Igarashi, A., Namba, T., *Catal. Commun.*, **4**, 243 (2003).
8) Mizuno, T., Yamada, H., Tagawa, T., Goto, S., *J. Chem. Eng. Japan*, **38**, 849 (2005).

要　　旨

反応抽出を用いたベンゼン部分酸化反応システム用触媒再生器の検討

山田　博史[†1)]，水野　友章[†1)]，田川　智彦[†1)]，Garun TANARUNGSUN[†2)]，
Piyasan PRASERTHDAM[†2)]，Suttichai ASSABUMRUNGRAT[†2)]

[†1)] 名古屋大学大学院工学研究科化学生物工学専攻分子化学工学分野，464-8603 名古屋市千種区不老町

[†2)] Center of Excellence in Catalysis and Catalytic Reaction Engineering, Dept. of Chemical Engineering, Chulalongkorn University, Bangkok 10330, THAILAND

ベンゼンの部分酸化反応によるフェノールの合成をベンゼン-水液2相系で行った。触媒としてVCl_3，酸化剤として気体酸素を用いた。反応システムは反応器，抽出器，触媒再生器の三つの装置からなる。反応器中において，ベンゼンは触媒の溶けている水相に溶け込みフェノールへと酸化される。生成したフェノールはベンゼン相に抽出され，それ以上の逐次酸化が抑制される。ベンゼン相に抽出されたフェノールはそのままではフェノールの蓄積に伴い水相に分配されて逐次酸化が進行してしまうので，抽出器において再度抽出され反応器系外に送られる。反応中に酸化されて失活した触媒を水素で還元し再生する触媒再生器について検討を行った。触媒再生器において還元触媒がない条件では触媒は再生されなかった。還元触媒としてPdはくを用いるとベンゼンの部分酸化反応は安定して進行した。また，停止-再起動も簡単に行うことができた。

Appendix 16

Submitted to Journal of Industrial and Engineering Chemistry

Type of Contribution: Research paper

Subject Area: - CHEMICAL REACTION ENGINEERING - REACTIONS

Ternary metal oxide catalysts for selective oxidation of benzene to phenol

Garun Tanarungsun [a], Worapon Kiatkittipong [b], Piyasan Praserthdam [a],

Hiroshi Yamada [c], Tomohiko Tagawa [c] and Suttichai Assabumrungrat [a,*]

[a] *Center of Excellence in Catalysis and Catalytic Reaction Engineering, Department of Chemical Engineering, Faculty of Engineering, Chulalongkorn University, Bangkok 10330, THAILAND*

[b] *Department of Chemical Engineering, Faculty of Engineering and Industrial Technology, Silpakorn University, Nakhon Pathom 73000, THAILAND*

[c] *Department of Chemical Engineering, Nagoya University, Chikusa, Nagoya, 464-8603, JAPAN*

* Corresponding author Tel.: +66 2 2186868; Fax: +66 2 2186877

E-mail address: Suttichai.A@chula.ac.th (S. Assabumrungrat)

Abstract

This paper studied the liquid phase hydroxylation of benzene to phenol with hydrogen peroxide catalyzed by ternary metal oxide catalysts (Fe(III), V(V) and Cu(II)) supported on TiO_2 at room temperature. The effects of V(V) and Cu(II) metal oxide loading were investigated. The catalysts were prepared by co-impregnation method and characterized by BET, XRD, XRF, SEM-EDX, NH_3-TPD techniques. It was reported that the presence of V(V) and Cu(II) influenced the acid property on the catalyst. The increase of the metal loading increased the acidity of the catalyst. TiO_2 loaded with Fe, V and Cu of 5, 2.5 and 2.5 wt%, respectively offered the highest yield of phenol. Although the increase of the metal loading improved the yield of phenol, the TOF reduced due to the reduction of dispersion of the catalyst metal. The optimum condition for the system is a reaction time of 4 h, catalyst weight of 0.2 g, the H_2O_2: benzene molar ratio of 2 and 6.25 g of ascorbic acid per mole of benzene.

Keywords*: Oxidation of benzene; Phenol production; Hydrogen peroxide; Fe(III); V(V); Cu(II); TiO_2*

Introduction

Phenol is an important chemical used in many industries. More than 90% of phenol has been produced from the cumene process [1]. However, the industrial cumene process has several significant shortcomings: it is a multistage synthesis; the intermediate cumene hydroperoxide is explosive; there are ecological problems, and the production rate of the co-product acetone exceeds market demand [2]. The direct hydroxylation of benzene to phenol is an attractive alternative for phenol production.

Some homogeneous and heterogeneous catalytic systems consisting of Fenton's reagent have been investigated for the hydroxylation of benzene using H_2O_2 [3-7] or O_2 as an oxidant [7-9]. Oxygen gas is a more environmental-friendly oxidant than H_2O_2 but it still offers low conversion and yield of phenol. The use of homogeneous liquid phase oxidation catalyst like Fenton catalysts, Fe^{2+}/ Fe^{3+}, or other dissolved transition metal cations, such as Cu^{2+}, Mn^{2+}, V^{3+}, V^{5+} and Co^{2+} [10] has proven to be quite efficient. However, it necessitates a tight pH control to prevent precipitation and extra steps for the recuperation and the reuse of the catalyst. The alternative approach has been based on the development of solid catalysts, which feature efficiency as well as stability under the reaction conditions. For industrial processes, heterogeneous catalysts have some advantages over homogeneous catalysts such as catalyst recovery and recycling.

Many researchers studied the oxidation of benzene to phenol by using the transition metal oxide catalysts supported on TiO_2 [11-13], SiO_2 [13], Al_2O_3 [13,14], MCM-41 [1,6,15,16], SBA-15 [17], activated carbon [1,18], clay [10], heteropolyacid [19,20] and amorphous microporous mixed oxides [21]. The most popular transition metal oxides for the oxidation of aromatics are Fe, Cu and V. Miyahara *et al*. [8] studied liquid phase oxidation of benzene by various supported Cu. Among the

supported Cu catalysts studied i.e., Cu/SiO_2, Cu/Al_2O_3, Cu/SiO_2-Al_2O_3, Cu/MCM-41, Cu/HMCM-41, Cu-NaY, CuO-SiO_2 and CuO-Al_2O_3, the $CuO–Al_2O_3$ catalyst prepared by a co-precipitation method was found to be an effective catalyst for phenol production. However, the results showed relatively low phenol yield.

Phenol production from benzene and H_2O_2 was carried out using Fe, Cu, V supported on TiO_2 [11,12], activated carbon [1,18] and MCM 41 [1]. The conversion and selectivity of the metal oxide catalyst could be improved by adding second and third metal oxides to Fe/TiO_2 [13].

The development of new catalysts for the direct oxidation of benzene to phenol remains an attractive and important subject for the success of this process. In this study, the focus was on the improvement of the catalytic performance of Fe/TiO_2 catalyst by adding second and third metal oxides (V and Cu) at different compositions to the catalysts. In addition, various techniques were employed to characterize the synthesized catalysts. Finally, the effects of various operating parameters; i.e., the reaction time, the ratio of H_2O_2 to benzene, the amount of catalyst, the amount of ascorbic acid, were investigated.

Experimental

Materials and chemicals

Table 1 summarizes the details of materials and chemicals employed in this work. All chemicals were used without further purification.

Catalyst preparation

Catalysts were prepared by impregnating TiO_2 with a mixed solution of metal precursors at 353 K. For example, 5 wt.% Fe, 2.5 wt.% V and 2.5 wt.% Cu loaded on TiO_2 (abbreviated as $Fe_5V_{2.5}Cu_{2.5}/TiO_2$) were prepared by mixing 9 g of TiO_2, 0.5 g of Fe (i.e. 3.17 g of iron (III) acetylacetonate), 0.25 g of V (i.e. 0.57 g of ammonium metavanadate (V)) and 0.25 g of Cu (i.e. 0.91 g of cupric (II) nitrate). The solution was then evaporated and dried for overnight. The obtained catalysts were calcined under a continuous feed of air (60 cm^3/min) in a furnace whose temperature was increased from room temperature to 773 K at a heating rate of 10 K/min and held for 5 h to remove the organic residues. After calcinations, the catalysts were stored in a dessicator.

Characterization

XRD patterns of the TiO_2 support and metal supported catalysts were obtained by using X-ray diffractrometer, D 5000 (Siemens AG) using Cu Kα radiation equipped with Ni filter with a detection range of 2θ = 20-80 and a resolution of 0.04.

BET surface area and porosity of the catalysts were measured by Micromeritics ASAP 2020.

XRF was performed to determine the bulk composition of catalysts. The analysis was performed using Siemens SRS3400. The composition of the catalyst samples was obtained as metal oxide using XRF analysis. Then it was recalculated as metal and presented in Table 2.

Ammonia-temperature programmed desorption (NH_3-TPD) was carried out in a Micromeritics 2000 TPD/TPR instrument. A catalyst sample (0.1 g) was treated at

523 K for removing water and degassing in a helium flow for 1 h and then saturated with a flow of 15% NH_3/He mixture after cooling to room temperature. After purging with helium at room temperature for 1 h to remove weakly physisorbed NH_3, the sample was heated to 1023 K at a rate of 10 K/min in a helium flow (30 cm^3/min).

FTIR spectra were recorded on a Nicolet impact 6700 instrument, in the range of 650-4000 cm^{-1} and with a spectral resolution of 4 cm^{-1}. Each sample was mixed with KBr with a sample: KBr ratio of 1:100 and then pressed into a thin wafer.

Scanning electron microscopy (SEM - JEOL JSM-5800LV), operated using the back scattering electron (BSE) mode at 20 kV and Energy dispersive X-ray spectroscopy (EDX - Link Isis Series 300 software) were used to determine the morphology and elemental distribution of the catalyst samples.

Experimental setup and product analysis

The oxidation of benzene by H_2O_2 was carried out in a 125-cm^3 round flat bottomed flask at 303 K and at a pressure of 1 atm with a high speed stirrer. The reaction system consisted of two liquid phases: an organic phase containing benzene and acetonitrile, and an aqueous phase containing acetonitrile and 30 wt% H_2O_2.

In typical experiment, 0.2 g of catalyst was added to a liquid mixture containing 40 cm^3 of acetonitrile, 30 cm^3 of H_2O_2 (0.32 mol) and 11 cm^3 of benzene (0.16 mol). Note that a preliminary study was carried out to investigate the effect of mass transfer resistance by varying the stirring speed (the results are not shown here). The conversion increased with increasing speed and, finally, leveled off at a speed of 600 rpm. Therefore, a speed of 600 rpm was used to ensure negligible mass transfer resistance in this study.

The feed and products were analyzed by a gas chromatography (GC 9A, Shimadzu Corp.) with a packed column of GP 10% SP-2100. The injection and detector temperatures were 523 K. The initial and final column temperatures were 383 K and 443 K, respectively with a temperature programmed rate of 10 K/min. The products were also analyzed by GC-MS (Agilent Technologies 6890 N Network GC system and 5973 Mass selective Detector) especially for some product species which cannot be detected by the FID detector.

The terms of reaction performance were defined as follows.

$$\text{Conversion of benzene} = \frac{\text{mole of benzene reacted}}{\text{initial mole of benzene}}$$

$$\text{Selectivity of phenol} = \frac{\text{mole of phenol produced}}{\text{mole of benzene reacted}}$$

$$\text{Yield of phenol} = \frac{\text{mole of phenol produced}}{\text{initial mole of benzene}}$$

$$\text{Turn over frequency (TOF)} = \frac{\text{mole of phenol produced}}{\text{mole of metal catalyst} \times \text{reaction time}}$$

Results and discussion

Catalysts

The formulas of catalysts with different percent metal loadings are abbreviated by using subscripts; for example, $Fe_5V_1Cu_1/TiO_2$ represents a catalyst with 5 wt% Fe and 1 wt% V and 1 wt% Cu loaded on TiO_2.

The chemical compositions of all catalysts were determined by elemental chemical analysis, by XRF and SEM-EDX as summarized in Table 2. XRF results representing the percent of metal loading in the bulk of catalyst showed that Fe was

mostly lower than 5 wt% loading. Vanadium showed higher percent metal loadings than calculations while copper showed the opposite trend likely due to the difficulty for copper to diffuse inside the support pores during the catalyst preparation. The analysis of percent loading on the surface by SEM-EDX showed that the percent loadings were close to those results from the XRF analysis. It should be noted that although the observed values of percent metal loading are different from the calculated values, they were usually increased when the catalysts were prepared with a higher percent of metal loading. Regarding the textural properties of the samples, the specific surface area of catalysts was remarkably decreased at high ratios of Cu/Fe and V/Fe loading as shown in Table 3.

The XRD patterns of the catalysts and the blank TiO_2 support were determined (not shown). However, no obvious peaks of Fe, Cu and V metals were observed when compared with the pattern of the blank TiO_2 even at a high range of metal loading. This observation was similar to the previous work [11]. FTIR spectra of the catalysts were recorded; however, no different peaks were observed (the results are not shown here). Both the acidity and the distribution of the acid strength of the catalysts were determined by the NH_3-TPD. As shown in Figure 1, only one peak ($T \approx 443$ K) was observed for Fe/TiO_2. However, when second and third metals were loaded on the catalyst, the acid properties of the catalyst were changed. A new peak at a lower temperature ($T \approx 373$ K) was observed in $FeCu/TiO_2$, FeV/TiO_2 and $FeCuV/TiO_2$ catalysts. The peak observed in the Fe/TiO_2 at $T \approx 443$ K disappeared but there are more peaks present at higher temperatures. The peaks at high temperatures may be contributed from the decomposition of the adsorbed ammonia. Regarding the percent loading of V and Cu, it is likely that the acidity of the catalyst should be higher when

the percent loading was increased as observed by the broadening of the low temperature peak.

Effect of operating parameters on the hydroxylation of benzene to phenol

Influence of reaction time

As shown in Figure 2, the yield of phenol increased with reaction time until 4 h. Then, it decreased especially in the case of high metal loading. The hydroxyl radicals are produced from the interaction of H_2O_2 with the catalyst. The reaction occurs similar to Fenton chemistry, through the participation of hydroxyl radical in the activating benzene toward the formation of phenol. Increasing the reaction time increased the concentration of phenol in the system; and then, phenol could be further oxidized to other byproducts (benzoquinone, hydroquinone and catechol) at higher reaction time, resulting in the decrease of the phenol concentration [11]. According to the above results, the reaction time of 4 h will be used in the subsequent studies. It should be noted that acetonitrile, which was employed as a solvent in this study, is not an inert solvent as reported by the study of Stockmann et al. [21]. Our preliminary blank test without benzene indicated that there were many products detected. However, fortunately, the phenol product was not obtained in the blank test without benzene as a reactant. Due to the great variety of byproducts from the reaction system, the quantitative analysis of the byproducts was not determined in this study.

Effect of percent loading of the second metal and the third metal

The mixed metal oxides with different ratios of metal supported on TiO_2 were tested in this work. The results summarized in Table 3 revealed that within the studied

ranges of percent loading of V and Cu, the multi metal oxide catalysts were more active for the hydroxylation of benzene to phenol than the Fe/TiO_2 although the increase of the percent loading of second metal and third metal decreased the BET surface area and pore volume particularly at high values of metal loading.

When Cu or V was loaded on the catalysts as in the cases of binary metal oxide catalysts ($Fe_5Cu_{2.5}/TiO_2$ and $Fe_5V_{2.5}/TiO_2$), the presence of the second metal significantly improved the conversion and TOF as reported in the previous work [11]. However, lower selectivity was observed for the case with Cu addition. The use of the second metal significantly improved the yield of phenol from 1.2% (Fe_5/TiO_2) to 5.96% ($Fe_5Cu_{2.5}/TiO_2$) and 6.31% ($Fe_5V_{2.5}/TiO_2$). When the third metal was loaded in the catalyst ($Fe_5V_{2.5}Cu_{2.5}/TiO_2$), the yield of phenol could be improved to 7.15% but the TOF was slightly lowered.

The effect of percent loading of second and third metal oxides was investigated. Both the percent metal loadings of V and Cu in the catalyst were at the same value for all catalysts. The percent loading of metal oxides obviously influenced the yield of phenol and TOF. The increase of the V and Cu loadings improved the benzene conversion; however, the phenol selectivity and TOF significantly reduced. The decrease of TOF at high metal loading could be due to the reduction of dispersion of the catalyst metal. The optimum percent loading of V and Cu which offered the highest phenol yield was 2.5 wt% ($Fe_5V_{2.5}Cu_{2.5}/TiO_2$) giving a phenol selectivity of more than 70%. The improved yield of phenol by the increase of metal loading was mainly contributed by the increase in the conversion. It is noted that the amounts of metal oxides in the catalysts have the effect on decomposition of H_2O_2 to hydroxyl radical and consequently the reactions taking place in the system.

Effect of the amount of catalyst

The effect of the amount of the catalyst was shown in Figure 3. It was found that increasing the amount of catalyst improved the conversion and phenol yield up to 0.5 g. However, further increasing of the amount of catalyst to 1 g decreased the yield of phenol for high V-Cu content, because increasing the amount of catalyst also increased the side reaction of phenol to other products.

The amount of catalyst had the effect on decomposition of H_2O_2 by Fenton reaction [11-12].

$$Fe(II) + H_2O_2 \longrightarrow Fe(III) + OH^{o} + OH^{-} \qquad (1)$$

The increased amounts of catalyst increased the amount of hydroxyl radical in the reaction which is necessary for the oxidation reaction of benzene to produce cyclohexadienyl (CHD) radical as follows.

$$OH^{o} + \text{benzene} \longrightarrow CHD \qquad (2)$$

$$CHD + Fe(III) \longrightarrow \text{phenol} + Fe(II) + H^{+} \qquad (3)$$

Although, the hydroxyl radical was very important for production of phenol, excessive hydroxyl radical can react with phenol to byproducts. In the selective oxidation of benzene to phenol, it is therefore essential to control the amount of hydroxyl radical per reactant.

Effect of the ratio of H_2O_2/benzene

As shown in Figure 4, it was found that the yield of phenol initially increased, leveled off and then decreased with the increase in the oxidant/benzene mole ratio. In the study, the volume of benzene remained constant while that of H_2O_2 changed. The conversion of benzene increased with the increased ratio of H_2O_2/benzene but the selectivity of phenol decreased because the amount of H_2O_2 influenced the amount of hydroxyl radical to react with benzene to hydroquinone, cresol and benzoquinone (not shown). The best value was observed at the ratio of H_2O_2/benzene of about 2 for all catalysts.

The use of high amount of H_2O_2 resulted in high amount of hydroxyl radical in the reaction. It increased the conversion and yield of phenol but excessive H_2O_2 caused a problem on further oxidation of phenol to byproducts.

Effect of the amount of ascorbic acid

Figure 5 shows the influence of the amount of ascorbic acid on the catalytic performance during the hydroxylation of benzene. The ascorbic acid is well known as a good reducing agent. It changes the state of metal catalyst from Fe(III) to Fe(II) or V(V) to V(IV) and Cu(II) to Cu(I) [8, 10-12]. The yield of phenol increased with the increase in the amount of ascorbic acid, but the use of large amount of ascorbic acid tended to inversely decrease the yield of phenol for all catalysts. The excessive amount of ascorbic acid promoted the decomposition of H_2O_2, resulting in higher amount of hydroxyl radical and consequently higher possibility for further oxidation of phenol to other byproducts.

In the cases of Cu and V, the formation of phenol proceeded through the similar mechanism as that of Fenton chemistry by replacing the redox of Fe(III)/Fe(II) to that of Cu(II)/Cu(I) as well as V(V)/V(IV). In the three phase reaction system, the reaction occurs in the aqueous polar phase. The catalyst-reducing agent is actually dissolved only in the water rich phase.

$$2\ Fe(III) + \text{ascorbic acid} + 0.5\ O_2 \longrightarrow 2\ Fe(II) + \text{Dehydroascorbic acid} + H_2O \quad (4)$$

$$2\ Fe(II) + O_2 + 2H^+ \longrightarrow 2Fe(III) + H_2O_2 \quad (5)$$

$$Fe(III) + H_2O_2 + H^+ \longrightarrow Fe(II) + OH^{o} + H_2O \quad (6)$$

Conclusion

The phenol synthesis from benzene and H_2O_2 catalyzed by FeVCu/TiO_2 with different values of metal loading was investigated. $Fe_5V_{2.5}Cu_{2.5}$ catalyst was found to offer the highest yield. The increase of the percent loading of the second metal and third metal improved the yield of phenol; however, the TOF decreased probably due to the lowering of dispersion of the catalyst samples at high values of metal loading. It was observed that the quantity of second and third metals also influenced the acid properties of the catalyst. The optimum condition for the system is: a reaction time of 4 h, catalyst weight of 0.2 g, the H_2O_2: benzene molar ratio of 2 and 6.25 g of ascorbic acid per mole of benzene.

Acknowledgements

Financial supports from the Thailand Research Fund and Commission on Higher Education are gratefully acknowledged.

References

[1] J. S. Choi, T. H. Kim, M. B. Saidutta, J. S. Sung, K. I. Kim, R. V. Jasra, S. D. Song, Y. W. Rhee, *J. Ind. Eng. Chem.*, **10**, 445 (2004).

[2] L. V. Pirutko, A. K. Uriarte, V. S. Chernyavsky, A. S. Kharitonov, G. I. Panov, *Micropo& Mesopo Mater.*, **48,** 345 (2001).

[3] T. Mizuno, H. Yamada, T. Tagawa, S. Goto, *J. Chem. Eng. Japan*, **38,** 849 (2005).

[4] D. Bianchi, M. Bertoli, R. Tassinari, M. Ricci, R. Vignola, *J. Mol. Catal. A.*, **200**, 111 (2003).

[5] A. Germain, M. Allian, F. Figueras, *Catal. Today*, **32**, 145 (1996).

[6] B. Chou, J. L. Tsai, S. Cheng**,** *Micropo& Mesopo Mater.***, 48,** 309 (2001).

[7] Y. K. Masumoto, R. Hamada, K. Yokota, S. Nishiyama, S. Tsuruya, *J. Mol. Catal. A.*, **184**, 215 (2002).

[8] T. Miyahara, H. Kanzaki, R. Hamada, S. Kuroiwa, S. Nishiyama, S. Tsuruya, *J. Mol. Catal. A.*, **176**, 141 (2001).

[9] H. Kanzaki, T. Kitamura, R. Hamada, S. Nishiyama, S. Tsuruya, *J. Mol. Catal. A.*, **208,** 203 (2004).

[10] X. Gao, J. Xu, *Appl. Clay Sci.*, **33**, 1 (2006).

[11] G. Tanarungsun, W. Kiatkittipon, S. Assabumrungrat, H. Yamada, T. Tagawa, P. Prasertdam, *J. Chem. Eng. Japan*, **40,** 415 (2007).

[12] G. Tanarungsun, W. Kiatkittipon, S. Assabumrungrat, H. Yamada, T. Tagawa, P. Prasertdam, *J. Ind. Eng. Chem.*, **13**, 444 (2007).

[13] G. Tanarungsun, W. Kiatkittipon, S. Assabumrungrat, H. Yamada, T. Tagawa, P. Prasertdam, *J. Ind. Eng. Chem.*, **13**, 870 (2007).

[14] K. Teramura, T. Tanaka, T. Hosokawa, T. Ohuchi, M. Kani, T. Funabiki, *Catal. Today.*, **96**, 205 (2004).

[15] V. Parvulescu, B.L. Su, *Catal. Today.*, **69**, 315 (2001).

[16] J. Okamura, S. Nishiyama, S. Tsuruya, M. Masai, *J. Mol. Catal. A*, **135**, 133 (1998).

[17] Y. Y. Gu, X. H. Zhao, G. R. Zhang, H. M. Ding and Y. K. Shan, *Appl. Catal A.*, **328**, 10, 150 (2007)

[18] J. S. Choi, T. H. Kim, K. Y. Choo, J. S. Sung, M.B. Saidutta, S. O. Ryu, S. D. Song, B. Ramachandra and Y. W. Rhee*, Appl. Catal A.*, **290**, 1 (2005)

[19] Y.J. Seo, Y. Mukai, T. Tagawa, S. Goto, *J. Mol. Catal. A*, **120**, 149 (1997).

[20] J.Zhang, Y. Tang, G. Li, C. Hu, *Appl. Catal. A*., **278**, 251 (2005).

[21] M. Stockmann, F. Konietzni, J.U. Notheis, *Appl. Catal. A.*, **208**, 343 (2001).

Table 1 Materials and chemicals.

Metal source	Iron (III) acetylacetonate 97% (Aldrich)
	Cupric (II) nitrate 99% (SIGMA)
	Ammonium metavanadate (V) 99.5% (Carlo Erba reagenti)
Support	TiO_2 (JRC-TIO1) (Catalysis Society of Japan)
Solvent	Acetonitrile 99.8% (MERCK)
Reducing agent	Ascorbic acid 99.7% (Polskic Odczynniki Chemiczne S.A.)
Substrate	Benzene 99.7% (MERCK)
Oxidant	Hydrogen peroxide 30% wt. (MERCK)
Byproduct reference	Biphenyl 99.9% (Fluka)
	Catechol 98% (Fluka)
	Phenol 99% (Panreac Sintesis)
	Quinol 99.8% (APS)
	1,4 Benzoquinone 98% (ACROS)

Table 2 Summary of metal loading determined by SEM-EDX and XRF.

	Metal loading by SEM-EDX (wt%)			**Metal loading by XRF (wt%)**		
Catalyst	**Fe**	**V**	**Cu**	**Fe**	**V**	**Cu**
1. Fe_5/TiO_2	4.36	-	-	4.59	-	-
2. $Fe_5V_1Cu_1/TiO_2$	5.87	1.84	2.51	4.31	1.43	0.65
3. $Fe_5V_{2.5}Cu_{2.5}/TiO_2$	4.31	2.39	2.11	4.2	2.65	1.95
4. $Fe_5V_5Cu_5/TiO_2$	3.66	6.83	3.17	4.29	8.55	3.01
5. $Fe_5V_{10}Cu_{10}/TiO_2$	3.68	8.73	3.47	3.97	13.44	6.49

Table 3 Experimental results of hydroxylation of benzene to phenol using different catalysts.

Catalyst	Conversion (%)	Selectivity (%)	Yield (%)	TOF (h^{-1})	BET (m^2/g)	Pore volume (cm^3/g)
1. Fe_5/TiO_2	1.5	80	1.20	2.68	69.3	0.26
2. $Fe_5Cu_{2.5}/TiO_2$	8.4	71	5.964	9.25	62.8	0.24
3. $Fe_5V_{2.5}/TiO_2$	7.6	83	6.308	9.11	55.3	0.21
4. $Fe_5V_1Cu_1/TiO_2$	6.6	85	5.61	8.98	66.2	0.23
5. $Fe_5V_{2.5}Cu_{2.5}/TiO_2$	9.8	73	7.154	8.04	65.9	0.22
6. $Fe_5V_5Cu_5/TiO_2$	11.7	61	7.137	5.36	42.1	0.17
7. $Fe_5V_{10}Cu_{10}/TiO_2$	14.8	49	7.252	3.27	39.6	0.16

(Benzene = 11 cm^3; catalyst weight = 0.2 g; benzene/H_2O_2 mole ratio = 0.5; acetonitrile solvent 40 cm^3; temperature = 303 K; pressure = 1 atm; reaction time = 4 h)

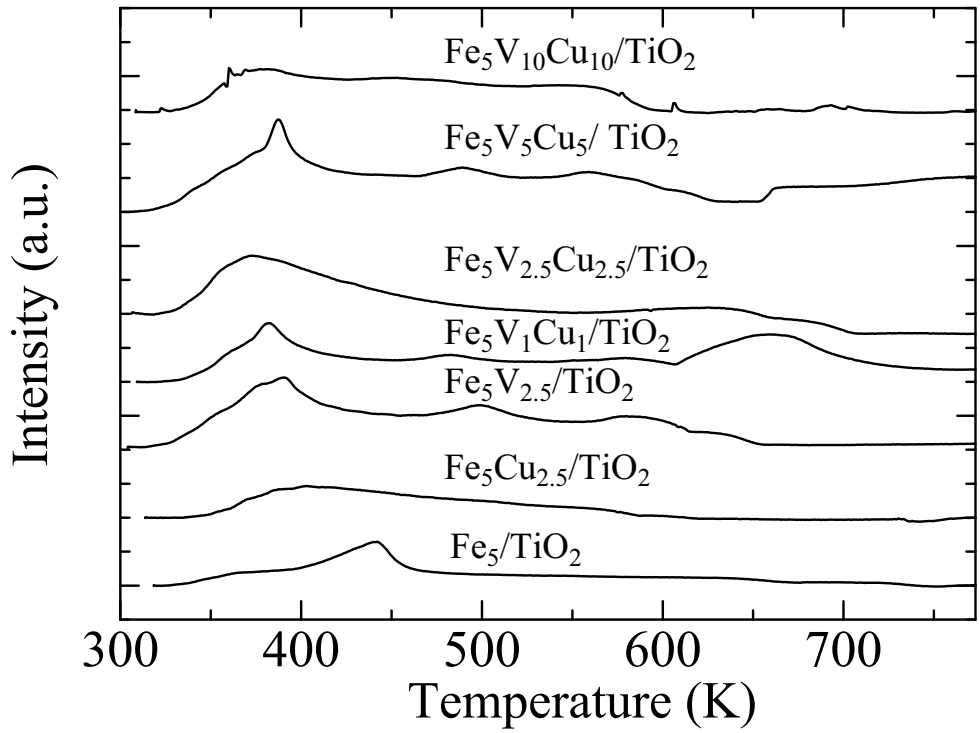

Figure 1 NH_3-TPD of different ternary metal oxide catalysts.

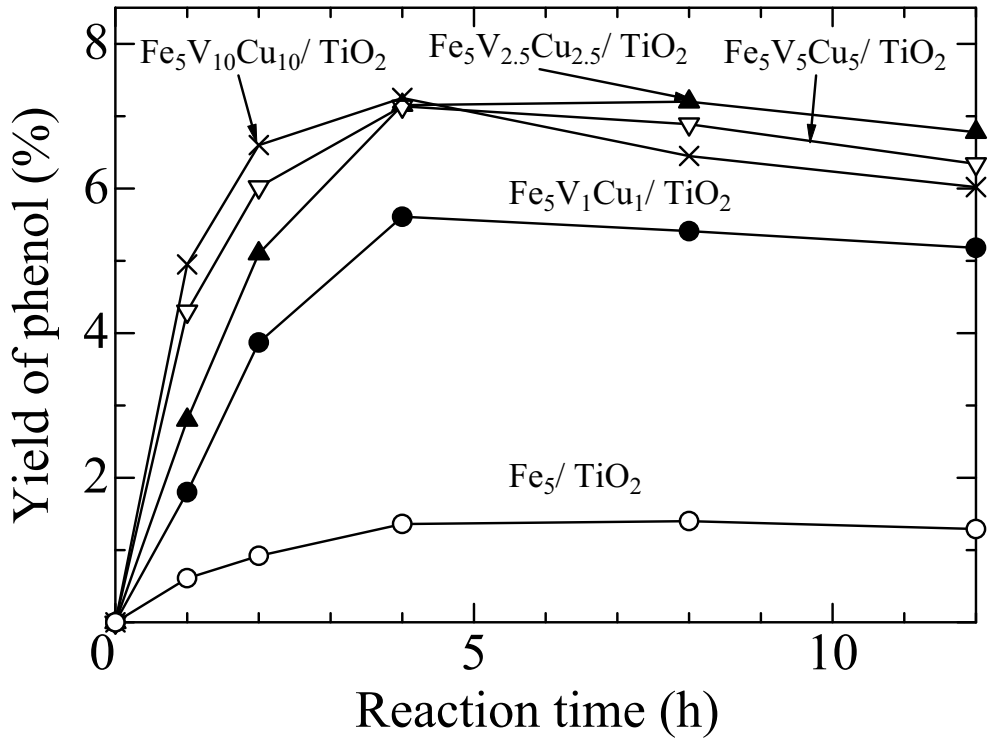

Figure 2 Influence of reaction time on yield of phenol.

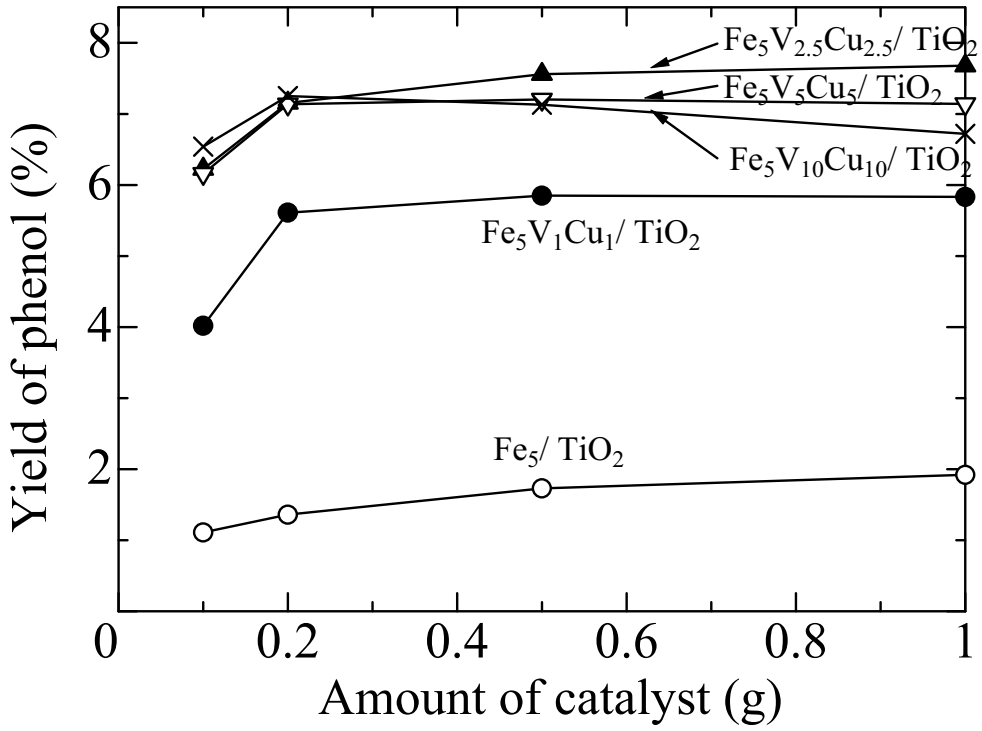

Figure 3 Influence of the amount of catalyst on yield of phenol.

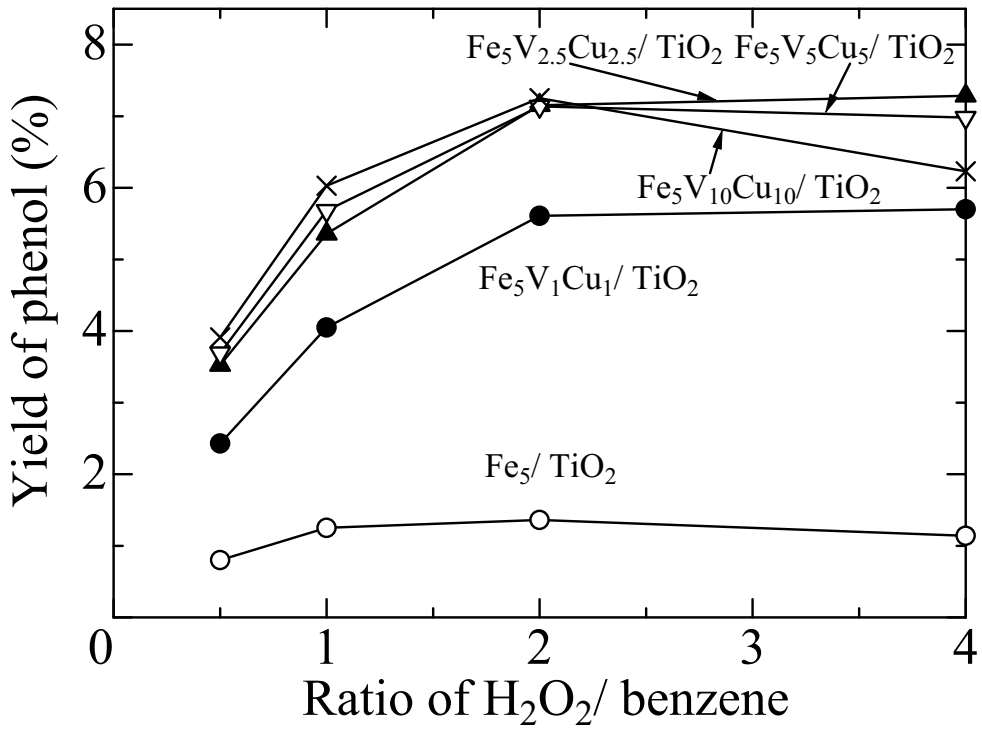

Figure 4 Influence of ratio of H_2O_2/benzene on yield of phenol.

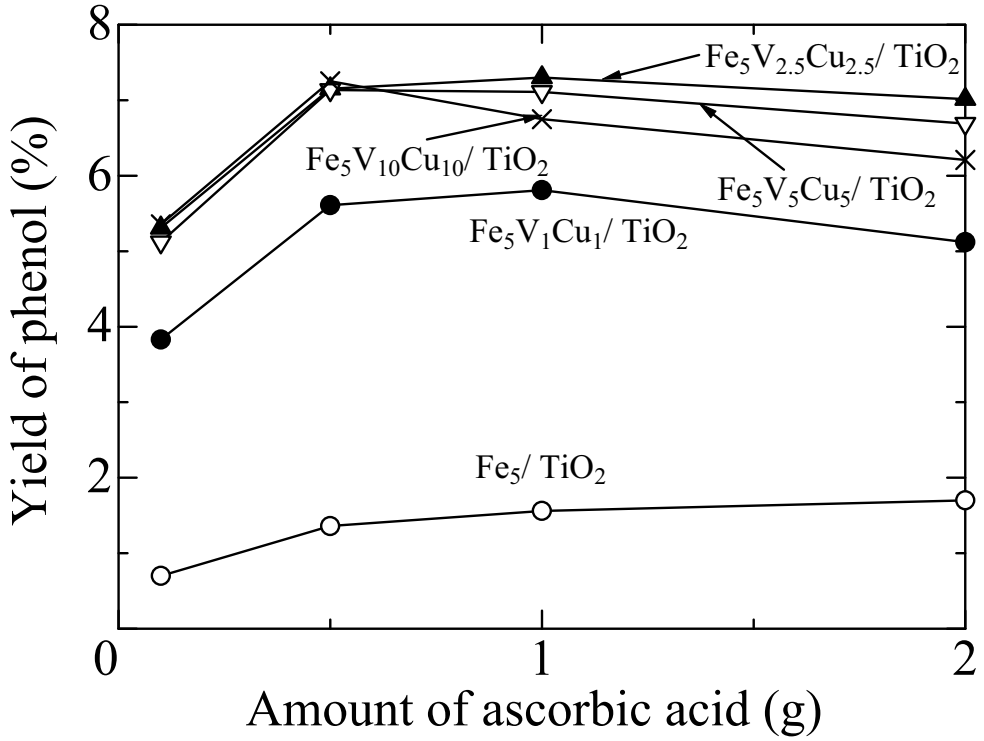

Figure 5 Influence of the amount of ascorbic acid on yield of phenol.

Appendix 17

Korean J. Chem. Eng., **24**(1), - (2007)

Carbon dioxide reforming of methane under periodic operation

Eakkapon Promaros, Suttichai Assabumrungrat†, Navadol Laosiripojana*, Piyasan Praserthdam, Tomohiko Tagawa and Shigeo Goto****

Center of Excellence in Catalysis and Catalytic Reaction Engineering, Department of Chemical Engineering, Faculty of Engineering, Chulalongkorn University, Bangkok 10330, Thailand
*The Joint Graduate School of Energy and Environment, King Mongkut's University of Technology Thonburi, Bangkok, 10140, Thailand
**Department of Chemical Engineering, Nagoya University, Chikusa, Nagoya, 464-8603, Japan
(*Received 30 May 2006 • accepted 28 August 2006*)

Abstract–The carbon dioxide reforming of methane under periodic operation over a commercial $Ni/SiO_2 \cdot MgO$ catalyst was investigated at two different temperatures, 923 and 1,023 K. According to this operation, pure methane and carbon dioxide were alternately fed to the catalyst bed where methane cracking and the reverse Boudouard reaction took place, respectively. Therefore, hydrogen and carbon monoxide products appeared separately in different product streams. The performance of this operation was compared to that of the steady state operation with simultaneous feed of both carbon dioxide and methane. At 1,023 K, the methane conversion and hydrogen yield from the periodic operation initially decreased with time on stream and eventually leveled off at values about half of those obtained in the steady state operation with co-feed of both reactants. The decreased catalytic activity was due to the accumulation of carbonaceous deposit and loss of metal active sites. However, a different trend was observed at 923 K. The methane conversion and hydrogen yield were almost constant over the time on stream, although more carbonaceous deposit was progressively accumulated on the catalyst bed during the reaction course. At this temperature, the periodic operation offered the equivalent hydrogen yield to the steady state operation. The observed behavior could be due to the different mechanisms of carbon formation over the catalyst. Finally, it was found that cycle period and cycle split did not influence the reaction performance within the ranges of this study.

Key words: Periodic Operation, Dry Reforming, Methane, Nickel Catalyst, Hydrogen

INTRODUCTION

Carbon dioxide reforming of methane is an effective way to produce synthesis gas and to utilize green house gases simultaneously. The reaction produces synthesis gas with low H_2/CO ratio, which is suitable for producing valuable chemicals such as alcohol, aldehyde and isobutene. Several supported transition metal catalysts (Ni, Ru, Rh, Pd, etc.) have been used for the carbon dioxide reforming of methane [Gadalla et al., 1988; Rostrup-Nielsen et al., 1993; Inui et al., 1997]. Nickel is well-known as an active catalyst for this highly endothermic reaction and mainly used in industry due to its low cost. A typical problem found for this reaction is catalyst deactivation due to the carbonaceous deposition, which is mainly generated from the following catalytic cracking of methane [Kim et al., 2003].

$$CH_4 \rightarrow C + 2\,H_2 \quad (1)$$

However, the presence of carbon dioxide theoretically helps the removal of deposited carbon according to the following reverse Boudouard reaction [Takano et al., 1996].

$$C + CO_2 \rightarrow 2CO \quad (2)$$

According to the above reactions, the carbon dioxide reforming of methane [Eq. (3)] can be operated periodically by feeding methane and carbon dioxide alternately.

$$CH_4 + CO_2 \rightarrow 2CO + 2\,H_2 \quad (3)$$

Under periodic operation, hydrogen and carbon monoxide are generated at different time, and therefore, these products can be directly separated without additional significant effort. This operation is attractive particularly in the case when carbon monoxide-free hydrogen is required for some applications as in a proton-exchange membrane (PEM) fuel cell. The periodic operation for this reaction is conceptually attractive; however, there is still no effort to demonstrate experimentally the benefit of the operation.

Although researches focusing on the use of carbon dioxide for removing deposited coke on catalysts are not widely performed, the uses of oxygen and/or steam are more common. It was reported that both oxidation with oxygen, and steam gasification could restore the catalytic activity of Ni-based catalyst after deactivation due to carbon formation [Zhang, and Amiridis, 1998]. In previous studies, Ni/SiO_2 catalyst could be fully regenerated at 923 K with steam for up to 10 successive cracking/regeneration cycles without any significant loss of catalytic activity [Aiello et al., 2000]. While the hydrogen production from cracking of methane over Ni guaze catalyst [Monnerat et al., 2001] could be optimized by operating reaction periodically with the catalyst regeneration in oxygen atmosphere under suitable period and cycle split. Moreover, the Ni/Al_2O_3 showed more activity with low carbonaceous deposition, by repeating many cracking/regeneration cycle (D-R treatment) [Ito et al., 1999] with carbon dioxide before using in reforming reaction.

†To whom correspondence should be addressed.
E-mail: suttichai.a@chula.ac.th

In this work, the periodic operation for the carbon dioxide reforming of methane was investigated. The operation involved two steps of 1) methane decomposition reaction and 2) catalyst regeneration via oxidation in carbon dioxide mixture of the deposited coke. The effects of operating variables of periodic operation such as operating temperature, cycle period (τ) and cycle split (s) on conversions of methane and carbon dioxide, and yield of hydrogen are investigated and compared to the results from steady state operation with simultaneous feed of both carbon dioxide and methane.

EXPERIMENTAL

1. Reaction Procedure

An industrial steam reforming catalyst, $Ni/SiO_2 \cdot MgO$, containing 55 wt% of nickel with surface area of 1.23×10^5 m^2/kg and nickel diameter of 44 nm was employed for the carbon dioxide reforming of methane in this research. A schematic diagram of the experimental setup, as shown in Fig. 1, consists of a gas feeding section, a fixed-bed reactor and an analytical section. High purity methane (99.999%) and carbon dioxide (99.999%) were used as the reactant gases. The feed was switched periodically between opening and closing by Solenoid valve (Flon industry, Japan), which was controlled by an on-off timer (Sibata BT-3). Argon was used for purging the system, and hydrogen was used for reducing catalyst before the experiment.

The reaction was carried out in a quartz tube fixed-bed reactor (internal diameter=0.011 m, length=0.5 m) heated by a temperature controlled electric oven. A thermocouple was placed in the furnace, at the level of the catalyst bed, to monitor temperature. A U-tube manometer, which was filled with silicone oil was positioned at the entrance of the reactor for indication of the pressure drop in the reactor, could be used as an emergency pressure relief valve. Experiments were performed using 0.3 g of $Ni/SiO_2 \cdot MgO$ catalyst, diluted with silicon carbide (1.0 g). The catalyst was reduced in a hydrogen flow (5×10^{-7} m^3/s) at 923 K for 1 h before use. The reaction was conducted at atmospheric pressure. The reactor effluent from periodic operation experiments was collected by a sample bag at the exit of the reactor. The sample product gas was analyzed with a TCD gas chromatograph (Schimadzu GC-8A, Japan) equipped with a Porapak-Q and Molecular Sieve 5A column. Argon was used as the carrier gas in the gas chromatograph with the flow rate of 0.5×10^{-6} m^3/s.

2. Catalyst Characterization

Spent catalyst from the deactivation and regeneration experiments was studied with a JEOL JSM-35CF scanning electron microscopy (SEM) that was operated by using the back scattering electron (BSE) mode at 15 kV. The XRD spectra of fresh and spent catalysts were measured by a SIEMENS D5000 X-ray diffractometer using Cu Kα radiation with an Ni filter in the 10-80° 2-θ angular region.

RESULTS AND DISCUSSION

1. Characteristics of Carbon Dioxide Reforming of Methane Under Periodic Operation

The behavior of the carbon dioxide reforming of methane under periodic operation was first investigated. In the first step, the catalytic cracking of methane [Eq. (1)] was carried out by feeding pure methane (4.167×10^{-7} m^3/s) to the catalyst bed operated at 1,023 K to determine the catalyst activity along time on stream of methane for 225 min. The methane conversion of $Ni/SiO_2 \cdot MgO$ was approximately 73% at the beginning and declined rapidly to about 50% within 25 min, Fig. 2. Then the conversion decreased to 15% after 50 min of reaction and fell slightly until the end of reaction. The U-tube pressure manometer indicated stable pressure drop in the first period of reaction. However, after 20 min, the pressure drop increased gradually until reaching a plateau in about 50 min of time on stream. It was revealed from the results that catalyst loses its activity due to carbonaceous deposition on the catalyst according to the methane cracking reaction, resulting in lowering conversion and increasing pressure drop within about 20 min.

After testing the catalytic activity of the methane cracking, we performed catalyst regeneration with carbon dioxide at the same operating temperature to investigate the time to restore spent catalyst. In this experiment, a spent catalyst after exposure in methane cracking for 25 min was used to prevent complete deactivation with coke formation. Significant amount of coke was accumulated in the catalyst bed after the methane cracking (not shown). The catalyst regeneration was performed by feeding pure carbon dioxide

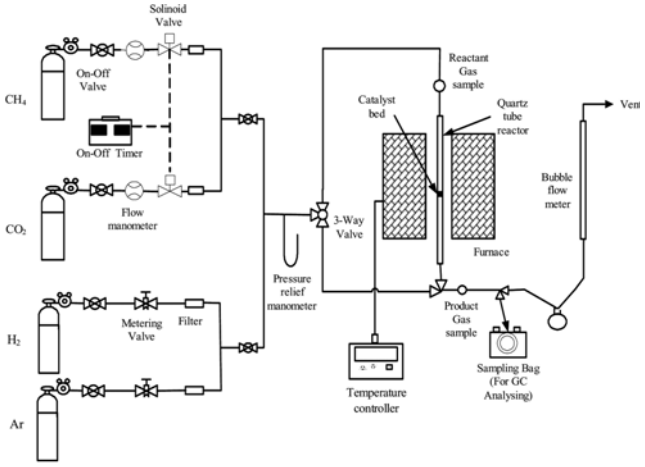

Fig. 1. Schematic diagram of the experimental setup for carbon dioxide reforming of methane under periodic operation.

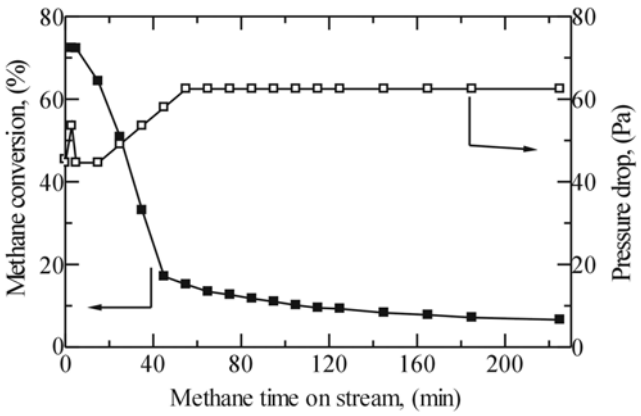

Fig. 2. Changes in catalytic activity and pressure drop of the catalytic cracking of methane over $Ni/SiO_2 \cdot MgO$ (T=1,023 K and methane flow rate=4.167×10^{-7} m^3/s).

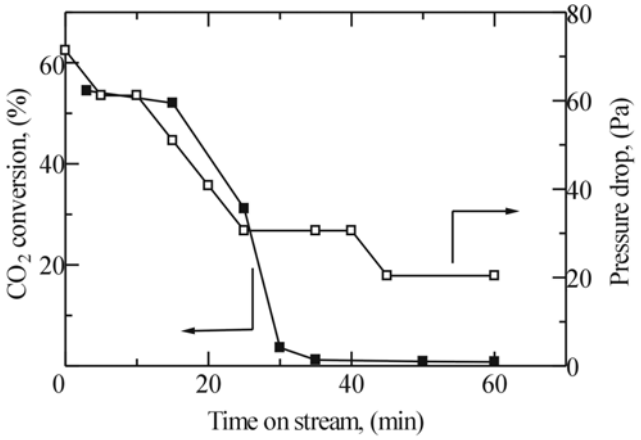

Fig. 3. Changes in CO_2 conversion and pressure drop over spent Ni/SiO_2·MgO catalyst after 25 min of methane cracking (T= 1,023 K and CO_2 flow rate=4.167×10^{-7} m^3/s).

(4.167×10^{-7} m^3/s) to the catalyst bed. Only carbon monoxide was detected as a main product according to the reverse Boudouard reaction [Eq. (2)].

Fig. 3 shows that the conversion of carbon dioxide was stable at about 54% for 20 min and then decreased steeply to about 3% after 30 min of time on stream of CO_2. Pressure drop decreased gradually from 60 Pa to 30 Pa in about 25 min, and declined slightly until the feed was stopped. It is expected that most of deposited coke could be removed from the spent catalyst within about 20 min of the regeneration step by reacting with carbon dioxide. From the above results, further studies were performed using a cracking period not to exceed 20 min for preventing complete deactivation of catalyst. Moreover, the regeneration period with carbon dioxide was not kept longer than 20 min to allow efficient utilization of carbon dioxide.

2. Performance Comparison of Carbon Dioxide Reforming of Methane Under Periodic and Steady State Operations

Performance comparison was considered for two cases of interest: steady state operation and periodic operation. All experiments were conducted at 1,023 K, atmospheric pressure and total reaction time of 200 min. For the steady state operation, a mixture of methane (2.083×10^{-7} m^3/s) and carbon dioxide (2.083×10^{-7} m^3/s) was allowed to flow through the catalyst bed in the reactor, whereas the periodic operation experiments were performed using a constant cycle split (s) of 0.5 and the flow rate of each reactant was kept at (4.167×10^{-7} m^3/s). The cycle split is defined as the duration of the cracking period divided by the duration of the cycle period (τ). In this study the cycle period (τ) was varied from 40 min (5 cycles) to 20 min (10 cycles), and 10 min (20 cycles). It should be noted that the time-average feed flow rates were equivalent in all experiments; therefore, the performance comparison was based on the same average feed rate or time on stream. Fig. 4 shows the profiles of methane conversion with time on stream for both steady state and periodic operations. It should be noted that the methane conversion of the periodic operation was time-average conversion calculated from average composition of gas product collected after the end of each cracking/regeneration cycle. It was found that the steady state operation offered a stable methane conversion at 90%, indicating no significant deactivation at least within 200 min of time on stream. In contrast, the periodic operation showed an initial conversion of about 80% which was around 10% lower than that of the steady state operation. The conversion further decreased and became stable after approximately 160 min of time on stream. It is obvious that the methane conversion from the periodic operation was inferior to that of the steady state operation over all ranges of reaction time.

The profiles of carbon dioxide conversion with time on stream are shown in Fig. 5. Similar to the previous results, the carbon dioxide conversion from the steady state operation (85%) did not change with time on stream, whereas the carbon dioxide conversion from the periodic operation decreased with increasing repeating cracking/regeneration cycles and then leveled off at high reaction cycles. However, after 160 min of time on stream the rates of coke formation and the coke removal seemed to be equivalent as the conversions of methane and carbon dioxide became nearly the same at around 40%; consequently, the conversions for both reactants no longer changed with reaction time. The profiles of hydrogen yield are shown in Fig. 6.

Clearly, periodic operation offered much lower hydrogen yield

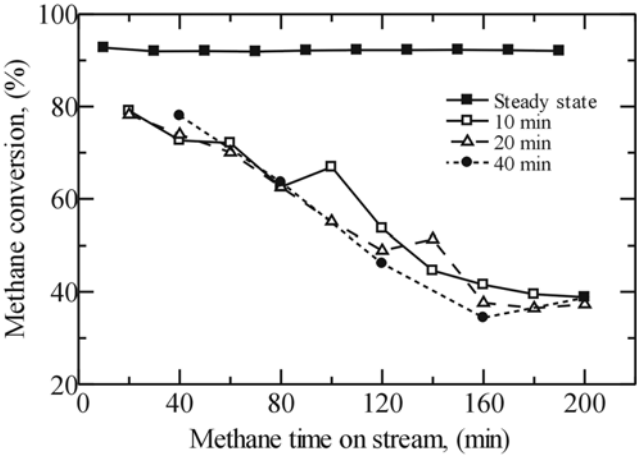

Fig. 4. Comparison of methane conversion between steady state operation and periodic operation at different cycle periods over Ni/SiO_2·MgO catalyst (T=1,023 K).

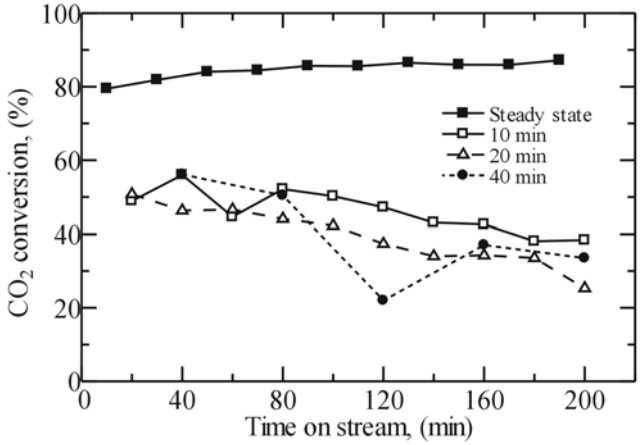

Fig. 5. Comparison of CO_2 conversion between steady state operation and periodic operation at different cycle periods over Ni/SiO_2·MgO catalyst (T=1,023 K).

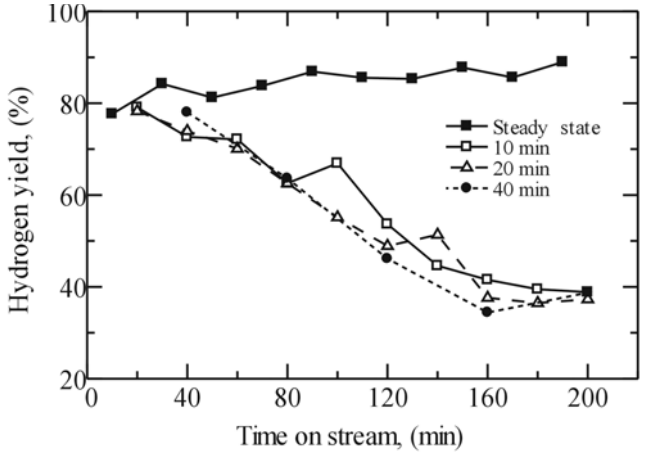

Fig. 6. Comparison of hydrogen yield between steady state operation and periodic operation at different cycle periods over Ni/SiO_2·MgO catalyst (T=1,023 K).

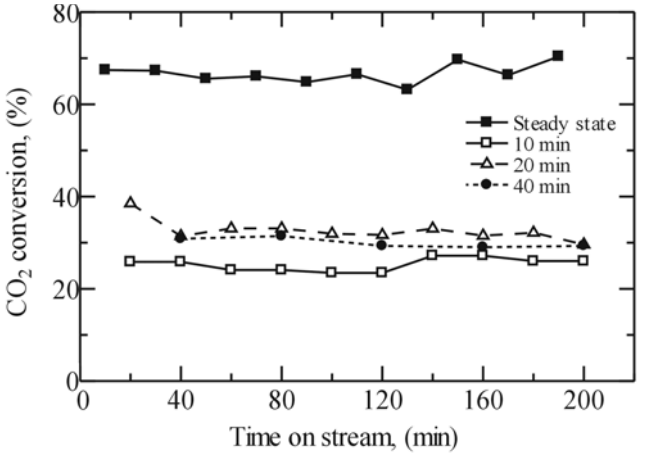

Fig. 8. Comparison of CO_2 conversion between steady state operation and periodic operation at different cycle periods over Ni/SiO_2·MgO catalyst (T=923 K).

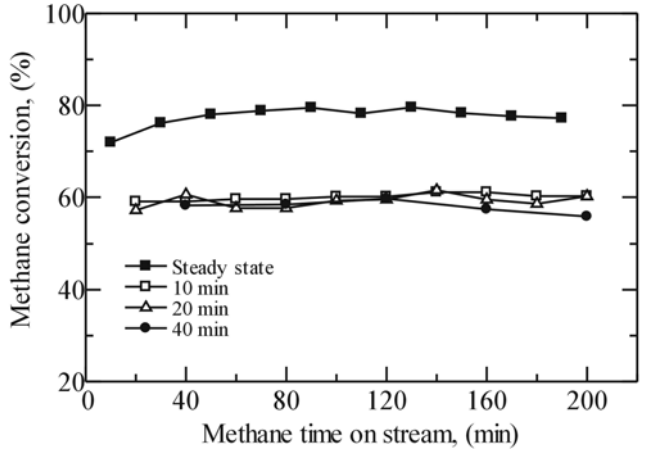

Fig. 7. Comparison of methane conversion between steady state operation and periodic operation at different cycle periods over Ni/SiO_2·MgO catalyst (T=923 K).

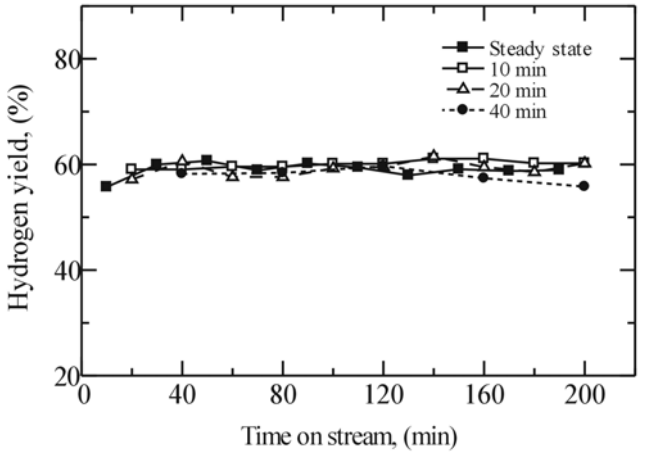

Fig. 9. Comparison of hydrogen yield between steady state operation and periodic operation at different periods over Ni/SiO_2·MgO catalyst (T=923 K).

than steady state operation. The experimental results at different cycle periods (τ=40, 20 and 10 min) indicate that the cycle period does not pronouncedly affect the reaction performance, Figs. 4-6. At higher cycle period, although the catalyst highly deactivated due to the formation of coke during the methane cracking step, more coke can be removed during the regeneration step. Therefore, the average reaction performance does not change significantly.

Another set of experiments was performed using operating conditions similar to the previous study, except that the temperature was changed from 1,023 K to 923 K. Figs. 7, 8 and 9 show the profiles of methane conversion, carbon dioxide conversion and hydrogen yield with time on stream at 923 K, respectively. The result indicates that for the steady state operation, the methane conversion at 923 K was also stable but the activity is about 10% lower than that at 1,023 K. This should be due to the lower reaction rate and less thermodynamic feasibility at lower temperature. For the periodic operation it was found that the methane conversion at 923 K was also stable at approximately 60% and independent of the cycle period. However, unlike the operation at 1,023 K, no indication of activity loss was detected at this operating temperature.

The profiles of carbon dioxide conversion with time on stream for both steady state and periodic operation at 923 K (Fig. 8) also show stable conversions at approximately 70% and 25-30%, respectively. Considering the obtained hydrogen yield (Fig. 9), it was found that the periodic operation provided hydrogen yield as high as that of the steady state operation, indicating equivalent performance of periodic operation at 923 K. Based on these results, the periodic operation seemed to become an attractive operation mode at 923 K regarding the equivalent hydrogen yield and stable performance as well as the capability to separate product streams of hydrogen and carbon monoxide.

According to the measurement of carbon deposition on the catalyst surface after exposure in the periodic operation at 923 K by comparing the conversions of methane and carbon dioxide, the results surprisingly indicate that more coke was further accumulated in the catalyst bed after each cracking/regeneration cycle. The unusual stable reaction activity throughout the reaction course at 923 K, which was in contrast to the behavior at 1,023 K reported earlier, was then

further investigated. Scanning electron microscopy (SEM) technique was used to observe the differences between catalyst samples that were subjected to 10 cracking/regeneration cycles (τ=20 min) with reaction temperature 923 K and 1,023 K, as well as a fresh catalyst sample. Both micrographs of the spent catalysts at 923 K (Fig. 10d) and 1,023 K (Fig. 10c) show the surface to be covered with filamentous carbon, in contrast to the clean surfaces of fresh catalyst (Figs. 10a and 10b).

In order to understand this dissimilar behavior, an X-ray diffraction technique was chosen to identify the crystal structure of Ni metallic and other metal forms on the catalysts. The characterizations were performed for the spent catalysts obtained after the periodic operation experiments at 923 K (τ=10 and 20 min) and 1,023 K (τ=10 min) with the cycle split (s) of 0.5. Measurements of the fresh catalyst and the spent catalyst after the steady-state operation at 923 and 1,023 K were also carried out for comparison. The XRD patterns, shown in Fig. 11, indicate that nickel contained in the fresh catalyst has crystal structure of NiO (peaks at 2θ=37.1, 43.1 and 62.7), which would be reduced with hydrogen to convert nickel oxide into the metallic nickel before the reaction is started. It also shows that the presence of carbon of graphitic nature, evident from the strong peak at 2θ=26, was accumulated in the fresh catalyst sample as well as carbon accumulated in the spent catalysts. Considering the spent catalyst from the periodic experiment with a cycle period (τ) of 20 min at 1,023 K, the strong peaks of Ni metallic crystallites at 2θ=44.5, 51.8, and 76.4 were observed with only small intensity of NiO peaks. It was presumed that NiO in the fresh catalyst could be completely reduced to metallic form after pre-reduction step. For the spent catalysts at lower temperature (923 K), the XRD patterns of the spent catalysts with τ=10 and 20 min indicated the existence of NiO peaks with lower Ni metallic intensity. It was suggested that NiO could be formed during the cracking/regeneration period and considered to be the active components for cracking period at 923 K. The XRD patterns of the spent catalysts from the steady-state operation for both temperature levels also indicate results similar to those of the periodic operation. Therefore, it is evident that the metal active sites involved in the reaction are in different form depending on the operating temperature.

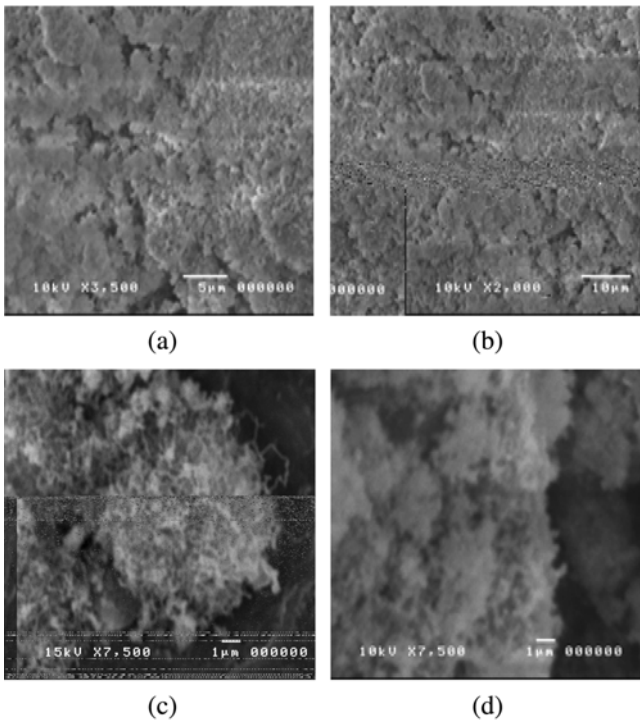

Fig. 10. SEM Micrograph of (a) and (b) fresh catalyst, (c) spent catalyst at 1,023 K, and (d) spent catalyst at 923 K after 10 successive cracking/regeneration cycles.

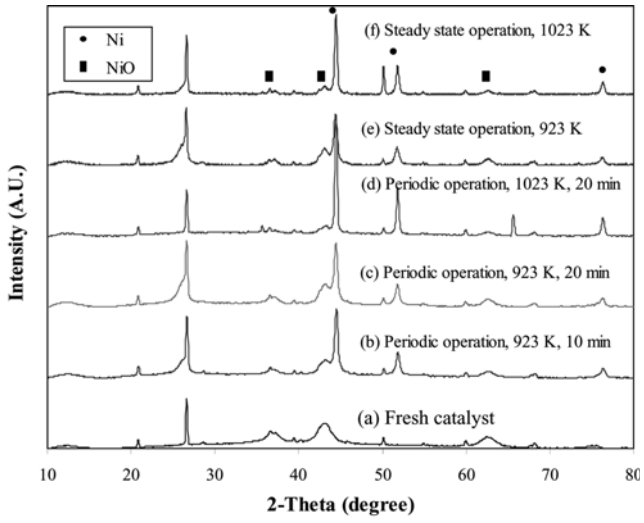

Fig. 11. XRD spectra of fresh catalyst and spent catalysts.

It can be concluded that, according to the different operating temperature and form of metal active site, the mechanisms of coke formation are different. Many researchers have suggested that the main type of carbon species which would be formed during the cracking period at high temperature was carbon whisker [Kuijpers et al., 1981; Poirier et al., 1997]. In the early stages of the deposition step, deposited carbon filaments could detach small nickel cores from bulk nickel on support. Then, the detached nickel cores which act as a growing core of whisker carbon could still accelerate the rate of carbonaceous deposition and increase their length with time on stream. After switching to the regeneration step, the carbon filaments are burned out with carbon dioxide and the nickel particles fall on the surface. The small nickel particles removed by regeneration may become inactive after the next cracking steps. Based on this suggestion, at a reaction temperature of 1,023 K, it may be stated that the growth of new carbon filaments could be terminated as a result of losing nickel active sites and no accumulation of carbon whisker on catalyst surface would occur during repeating cracking/regeneration. Consequently, the methane conversion decreased with time on stream as clearly shown in Fig. 4.

Considering the experimental results at 923 K, the formation of carbon filament was expected to be hindered by the low solubility of carbon in metal particle at low temperature. Moreover, the strong interaction between surface oxygen and metallic Ni, which results in formation of NiO in periodic operation at 923 K, was suggested to terminate the diffusivity of carbon into the nickel. These should be the cause of the different type of carbon formation at 923 K. In addition, the coke formed on the metal active sites may further move to the catalyst support, according to the drain-off phenomena that

has been reported in some reaction systems. Therefore, the accumulation of coke on the catalyst could not hinder the catalyst activity, at least within a reaction time of 200 min in this study. It should be noted that more detailed study on the Ni forms and coke formed is required to understand the behavior of the reaction system under periodic operation. It is suggested that the characterizations should be carried out separately at each reaction step of periodic operation and that operation with inert purge gas fed between each reaction step would provide additional useful data for understanding the behaviour of periodic operation.

In practical operation, it is desired, for periodic operation, that coke formation be kept as low as possible to avoid catalyst deactivation. Therefore, another set of experiments was carried out at 923 K with various values of cycle split (s). The cycle period was fixed at 20 min and the time-average flow rates of the reactant gases were kept at the same values as described earlier. It is expected that due to the slow rate of catalyst regeneration by carbon dioxide, the increase of regeneration period by lowering the feed flow rate of carbon dioxide (in order to keep the same average carbon dioxide flow rate) should help to increase the removal of coke arising from the methane cracking step and the corresponding reaction performance may be improved. The results for the cycle split (s) of 0.25, 0.4 and 0.5 are shown in Figs. 12 and 13. It was found that the decrease of the cycle split did not improve the reaction performance as expected. On the other hand, it slightly lowered both the methane and carbon dioxide conversions. This might be due to the shorter residence time during the methane cracking which caused the lower methane conversion. The decrease of carbon dioxide conversion should be due to the higher effect of mass transfer resistance at low reactant flow rate.

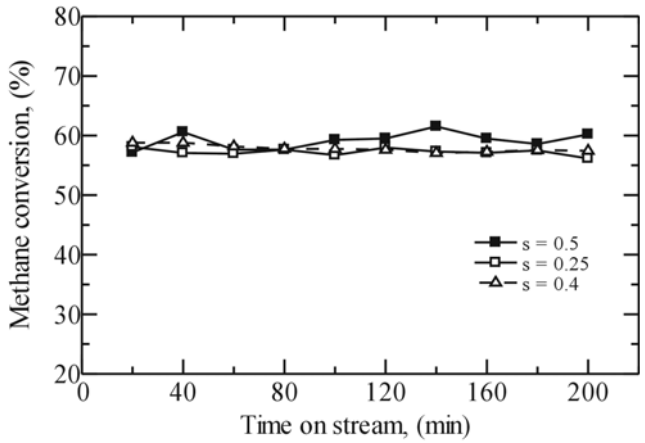

Fig. 12. Comparison of methane conversion between periodic operation at different cycle splits over Ni/SiO_2·MgO catalyst (T=923 K).

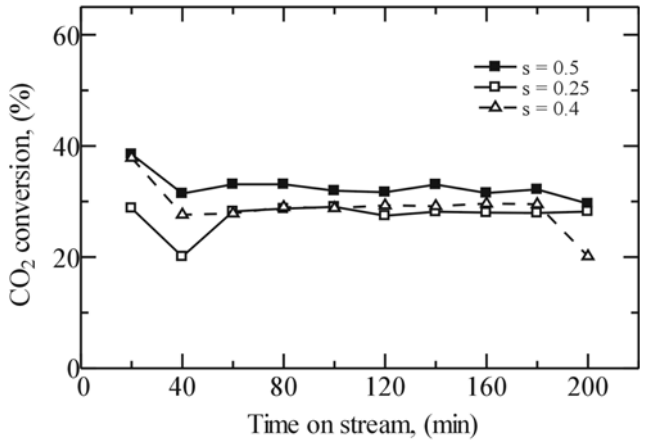

Fig. 13. Comparison of CO_2 conversion between periodic operation at different cycle split over Ni/SiO_2·MgO catalyst (T= 923 K).

CONCLUSIONS

Periodic operation was applied for the carbon dioxide reforming of methane. The effects of key parameters such as reaction temperature, cycle period and cycle split on the methane and carbon dioxide conversions and the hydrogen yield were investigated. By operating at the same time-average flow rates of the reactants, the results of the periodic operation were compared among different operating conditions and those of steady state operation. It was found that periodic operation was inferior to steady state operation at 1,023 K. However, at 923 K, the periodic operation offered the equivalent hydrogen yield of the steady state operation with an additional benefit on the separated hydrogen and carbon monoxide products in the different product streams. It was observed that the carbonaceous deposit was progressively accumulated in the catalyst bed during the course of reaction. Further studies are required to investigate the observed results in more detail.

ACKNOWLEDGMENTS

The support from The Thailand Research Fund, Commission on Higher Education, TJTTP-JBIC and the Graduate School of Chulalongkorn University is gratefully acknowledged. The authors also would like to thank Mr. Boonrat Pholjaroen for his technical assistance.

REFERENCES

Aiello, R., Fiscus, J. E., Loye, H.-C. and Amiridis, M. D., "Hydrogen production via the direct cracking of methane over Ni/SiO_2: Catalyst deactivation and regeneration," *App. Cat. A. Gen.*, **192**, 227 (2000).

Gadalla, A. M. and Bower, B., "The role of catalyst support on the activity of nickel for reforming methane with CO_2," *Chem. Eng. Sci.*, **11**, 3049 (1988).

Inui, T., Ichino, K., Matsuoka, I., Takeguchi, T., Iwamoto, S., Pu, S. B. and Nishimoto, S., "Ultra-rapid synthesis of syngas by the catalytic reforming of methane enhanced by *in-situ* heat supply through combustion," *Korean J. Chem. Eng.*, **14**, 441 (1997).

Ito, M., Tagawa, T. and Goto, S., "Suppression of carbonaceous depositions on nickel catalyst for the carbon dioxide reforming of methane," *App. Cat. A. Gen.*, **177**, 15 (1999).

Kim, M. H., Lee, E. K., Jun, J. H., Han, G. Y., Kong, S. J., Lee, B. K., Lee, T. J. and Yoon, K. J., "Hydrogen production by catalytic decomposition of methane over activated carbons: Deactivation study," *Korean J. Chem. Eng.*, **20**, 835 (2003).

Kuijpers, E. G. M., Jansen, J. W., Dillen, V. and Geus, J. W., "The revers-

ible decomposition of methane on a Ni/SiO_2 catalyst," *J. Catal.*, **1**, 75 (1981).

Monnerat, B., Kiwi-Minsker, L. and Renken, A., "Hydrogen production by catalytic cracking of methane over nickel gauze under periodic reactor operation," *Chem. Eng. Sci.*, **56**, 633 (2001).

Poirier, M. G. and Sapundzhiev, C., "Catalytic decomposition of natural gas to hydrogen for fuel cell applications," *Int. J. of Hydrogen. Energy*, **4**, 429 (1997).

Rostrup-Nielsen, J. R., "Production of synthesis gas," *Cat. Today*, **4**, 305 (1993).

Takano, A., Tagawa, T. and Goto, S., "Carbon deposition on supported nickel catalysts for carbon dioxide reforming of methane," *J. Japan Prtro. Inst.*, **39**, 144 (1996).

Zhang, T. and Amiridis, M. D., "Hydrogen production via the direct cracking of methane over silica-supported nickel catalysts," *App. Cat. A. Gen.*, **167**, 161 (1998).

Appendix 18

Elsevier Editorial System(tm) for Fuel Processing Technology
Manuscript Draft

Manuscript Number: FUPROC-D-08-00116

Title: Reactivity of Ni/SiO2.MgO toward carbon dioxide reforming of methane under steady state and periodic operations

Article Type: Research Paper

Section/Category:

Keywords: Coke; dry reforming; hydrogen; periodic operation

Corresponding Author: Professor Suttichai Assabumrungrat, Ph.D.

Corresponding Author's Institution: Chulalongkorn University

First Author: Boonrat Pholjaroen , MEng

Order of Authors: Boonrat Pholjaroen , MEng; Navadol Laosiripojana , PhD; Piyasan Praserthdam , PhD; Suttichai Assabumrungrat, Ph.D.

Manuscript Region of Origin:

Abstract:

Suggested Reviewers: Tomohiko Tagawa
Professor
tagawa@nuce.nagoya-u.ac.jp

Eric Croiset
Professor, University of Waterloo
ecroiset@cape.uwaterloo.ca

Opposed Reviewers:

Department of Chemical Engineering

Faculty of Engineering

Chulalongkorn University

April 13, 2008

Dear Professor Liu (the editor of Fuel Processing Technology),

I would like to submit a research article entitled "Reactivity of $Ni/SiO_2.MgO$ toward carbon dioxide reforming of methane under steady state and periodic operations" for your consideration for inclusion in Fuel Processing Technology. The article is original and unpublished and is not being considered for publication elsewhere.

If you have any query, please do not hesitate to contact me. I am looking forward to hearing from you.

Sincerely yours,

(Professor Suttichai Assabumrungrat)
Department of Chemical Engineering, Faculty of Engineering,
Chulalongkorn University, Bangkok 10330, Thailand
Tel: 662-2186878-82; fax:662-2186877
E-mail: Suttichai.A@chula.ac.th

Submitted to: Fuel Processing Technology

Type of contribution: Research Article

Reactivity of $Ni/SiO_2.MgO$ toward carbon dioxide reforming of methane under steady state and periodic operations

B. Pholjaroen [a], N. Laosiripojana [b], P. Praserthdam [a] and S. Assabumrungrat [a,]*

[a] *Center of Excellence in Catalysis and Catalytic Reaction Engineering,*
Department of Chemical Engineering, Faculty of Engineering,
Chulalongkorn University, Bangkok, 10330, Thailand

[b] *The Joint Graduate School of Energy and Environment,*
King Mongkut's University of Technology Thonburi, Bangkok, 10140, Thailand

[*] Corresponding authors (Email: Suttichai.A@chula.ac.th)

Abstract

The carbon dioxide reforming of methane over commercial $Ni/SiO_2.MgO$ catalyst under periodic and steady state operations were investigated at a temperature range of 650-750ºC. Under steady state operation, methane conversions tended to be constant with reaction time and increased with increasing reaction temperature. It was then observed that, at low temperature (650ºC) under the periodic operation, methane conversion was also constant at approximately 48% throughout reaction time, but for the operation at a higher temperature i.e. 750ºC, higher methane conversion (about 67%) was initially achieved but decreased dramatically with reaction time (to 27% in 240 min). The reason for the catalyst deactivation particularly under the periodic operation was further investigated. It was suggested that, at different operating temperatures, various types of coke occurred on the surface of catalyst and affected the catalytic activity. It was also found that, at low temperature under periodic operation, greater amount of coke was formed as filamentous carbon during the methane cracking period and was incompletely removed during the regeneration period. However, the deposition of this type of coke did not significantly affect the activity of catalyst. In contrast, at high temperature, lesser amount of coke was obtained but in the form of encapsulating carbon which strongly affected the activity of catalyst and resulted in the rapid catalyst deactivation.

Keywords: Coke; dry reforming; hydrogen; periodic operation

1. Introduction

Synthesis gas can be produced from several sources of hydrocarbons via different reforming reactions, which permit variations in a H_2:CO ratio. Carbon dioxide reforming of methane is attractive from an environmental view point because this reaction reduces greenhouse gases i.e. methane and carbon dioxide, which are among the main cause of the global warming problem. In certain applications such as proton-exchange membrane (PEM) fuel cell, CO-free hydrogen is required as the feed. Although carbon dioxide reforming of methane in steady-state operation can produce hydrogen, the existence of carbon monoxide and carbon dioxide in product stream is the major drawback as it is difficult and requires a costly process to separate hydrogen from these gases. A way to solve this problem is the carbon dioxide reforming of methane operated periodically by feeding methane and carbon dioxide alternately. According to this process, the first step is the catalytic thermal cracking of methane, in which methane is converted to hydrogen and coke (Eq. 1). Carbonaceous deposition typically causes plugging and catalytic deactivation problems, and thus, the second step is then applied by feeding carbon dioxide in order to regenerate the catalyst via the reverse carbon monoxide disproportionation (Eq. 2).

$$CH_4 \rightarrow C + 2H_2 \quad (1)$$

$$C + CO_2 \rightarrow 2CO \quad (2)$$

From the periodic operation, pure hydrogen can be produced separately from further gaseous product e.g. carbon monoxide. In addition, this operation also offers

another potential benefit on the heat integration within the reactor; as the exothermic heat from the catalyst regeneration can supply for the endothermic methane cracking to generate hydrogen [1].

Numerous supported transition metal catalysts (Ni, Ru, Rh, Pd, etc.) have widely been applied for the dry reforming of methane [2-5]. Rostrup-Nielsen and Bak Hansen [6] investigated the activity toward this reaction. The order of reactivity for this reaction was Ru > Rh > Ni ~ Ir > Pt > Pd, similar to their proposed order for steam reforming. They also observed that the replacing of steam with carbon dioxide gave similar activation energies, which indicated a similar rate-determining step in these two reactions. Erdohelyi et al. [7, 8] studied the influence of the catalyst support on the carbon dioxide reforming of methane over rhodium-based catalyst, and reported that the support had no effect on the activity of Rh. In contrast, Nakamura et al. [9] and Zhang et al. [10] observed that the initial turnover frequency (specific activity) of Rh crystallities was significantly affected by their supports. Zhang et al. [10] also reported that the deactivation of Rh crystallities was strongly dependent on their supports. Based on several studies, noble metal based catalysts seem to be less sensitive to coking compared to nickel based catalysts; however, noble metals are expensive and of limited availability. Nickel catalyst which has lower cost is therefore attractive for the carbon dioxide reforming of methane under periodic operation.

In the present work, the performance of carbon dioxide reforming of methane under periodic operation over an industrial steam reforming $Ni/SiO_2.MgO$ catalyst was investigated and compared to that under steady state operation at reaction temperatures between 650-750°C. Details of the carbon formation taking place during this reaction

under periodic operation were investigated by various characterization methods i.e. TPO, XRD, and BET in order to understand the behavior of catalyst toward this operation at several reaction temperatures and times. Furthermore, several pre-characterizations i.e. TPR, CH_4-TPD, and CO_2-TPD were also performed to find the suitable operation and pretreatment conditions.

2. Experimental

2.1. Catalyst

A commercial-grade reforming catalyst of 55 wt%Ni/SiO_2.MgO supplied from Japan was used in the present work. The shape of catalyst was solid cylindrical extrudate with a diameter of 3 mm and also 3 mm in length. Silicon dioxide (SiO_2) supplied by Fluka was chosen as a dilution material in this research. The average size of SiO_2 was 40-100 mesh. The ratio of Ni/SiO_2.MgO catalyst to silicon dioxide was 0.3:1 in the whole experiment.

2.2. Apparatus and procedures for catalytic reforming testing

The reaction was performed in a quartz tube (inter diameter = 11 mm) at atmospheric pressure. The quartz tube reactor was placed in the vertical direction with downward gas flow. Catalyst was placed over quartz wool which was packed for supporting the catalyst bed. The tube furnace was connected with the automatic temperature controller to supply heat to the reactor. Reactor temperature was measured by a type-K thermocouple which was placed in the furnace at the close position to the

catalyst bed. The flow rate of each reactant gas was controlled by mass flow controller (GFC17S) operated under a flow range between 0-50 mL/min. For periodic operation, each reactant feed was switched between opening and closing alternately by using a solenoid valve (Flon industry, Japan) controlled by a multi-timer (Sibata BT-3). Fig. 1 shows the schematic diagram of this lab-scale testing system.

For the catalyst testing, the mixture of catalyst with SiO_2 (0.1314 g of Ni/SiO_2.MgO with 0.438 g of SiO_2) was packed in the middle section of the reactor and then placed in the furnace. The reactor was heated up to 650°C under 30 mL/min of argon flow. When the temperature reached 650°C, the argon gas was switched off. The catalyst was reduced under 30 mL/min of hydrogen flow for 1 h. After that, the system was purged with argon again for 10 min to remove all hydrogen gas from the system and the reactor temperature was changed to a desired value (550, 650, 670, 690, 710, 730 or 750°C). For steady state operation experiment, the reaction was started by introducing 12.5 mL/min CH_4 together with 12.5 mL/min CO_2 simultaneously. For periodic operation, the multi-timer was set to control the solenoid valves to allow 25 mL/min of CH_4 to pass through the reactor for 10 min and switch to 25 mL/min of CO_2 for 10 min. The operation occurred repeatedly until the end of experimental study.

The product composition was determined by gas chromatography (Shimadzu modal 8A (GC-8A) equipped with a thermal conductivity detector (TCD)). In case of steady state operation, product gas for each reaction time was sampled from the sampling point by a syringe, whereas the product gas from periodic operation testing was collected every 10 min by using a sampling bag. Gas sample from the sampling bag was then analyzed to determine the time-average composition of the product gas.

2.3. Characterization

In order to study the physical properties, both fresh and spent catalysts were characterized by several methods as described below:

2.3.1. Temperature-programmed reduction (TPR)

The reduction temperature of fresh catalyst was measured by TPR technique using Micromeritrics Chemisorb 2750 in order to determine the amount of hydrogen consumption in reducing catalyst. A sample of 0.2 g was pre-treated in He (30 mL/min) at 250ºC for 1 h and then cooled down to room temperature. H_2 (20 mL/min) was switched into the sample while the system was heated at a ramping rate of 10ºC/min to 1000ºC. The exit gas was detected by TCD and the amount of H_2 consumed for reducing the catalyst was calculated and reported by Chemisorp TPx software.

2.3.2. Temperature-programmed desorption with CH_4 and CO_2 (CH_4-TPD and CO_2-TPD)

Adsorption ability of methane on the surface of fresh catalyst was measured by CH_4-TPD technique to determine the amount of adsorbed methane on the surface, while the basic property and carbon dioxide adsorption ability were measured by CO_2-TPD technique using Micromeritrics Chemisorb 2750 to measure the amount of adsorbed carbon dioxide on the surface.

For the CH_4-TPD, a sample of 0.3 g was pre-treated in He (30 mL/min) at 250ºC for 1 h and then reduced in H_2 (30 mL/min) at 650ºC for 1 h for the purpose of adjusting

the same condition to the catalyst before reaction. CH_4 (30 mL/min) was switched into the sample at room temperature for 1 h and then He (30 mL/min) was fed to remove adsorbed CH_4 from the surface of catalyst while the system was heated at a ramping rate of 10ºC/min to 1000ºC. The exit gas was detected by TCD. The calculation of amount of CH_4 was done and reported by Chemisorp TPx software. Regarding CO_2-TPD, the same procedure as CH_4-TPD was applied; only CO_2 was used instead of CH_4.

2.3.3. Temperature-programmed oxidation (TPO)

Temperature-programmed oxidation was used to characterize coke deposited on the spent catalysts. The operation was performed by using Micromeritrics Chemisorb 2750. The spent catalyst from the reaction was firstly pre-treated in He (25 mL/min) at 250ºC for 1 h to eliminate moisture from the catalyst and cooled down to room temperature. Then 1 vol% oxygen in helium (15 mL/min) was switched into the sample while the system was heated at a ramping rate of 10ºC/min to 1000ºC and the exit gas was detected by a TCD detector. The calculation of amount of CO_2 in the effluent gas was analyzed and reported by Chemisorp TPx software.

3. Results and discussion

3.1. Characterization of fresh Ni/SiO_2.MgO Catalyst

TPR profile of the fresh catalyst is shown in Fig. 2. Three reduction peaks were observed at 190, 616, and 813ºC. The strong peak observed at 616ºC can be assigned to the reduction of Ni species with strong interaction with silicon dioxide support. The peak

at 813ºC is assigned to the reduction of Ni species with strong interaction with magnesium oxide. According to all experiments in the present work, the reduction temperature was 650ºC and, therefore, the metallic phase should be converted from nickel oxide to metallic nickel which is more active before the reaction test.

CH_4 temperature-programmed desorption (CH_4-TPD) of fresh catalysts was carried out in order to study the methane adsorption behavior on this type of catalyst. The samples were reduced in H_2 at 650ºC for 1 h prior to adsorption of CH_4 and then the adsorbed catalysts were purged with He at the same adsorption temperature to remove physisorption. The results shown in Fig. 3 indicate that methane adsorbs on the surface of $Ni/SiO_2.MgO$ at the temperature range of 600-1000ºC and the methane adsorption at reaction temperature of 750ºC is significantly higher than that at 650ºC. Thus, the methane conversion at 750ºC should be higher than that at 650ºC.

It was proposed that basic property of catalyst improves activity of CO_2 reforming reaction. The effect of the surface basicity of the catalysts was studied by CO_2-TPD. The CO_2-TPD profile of $Ni/SiO_2.MgO$ is presented in Fig. 4. Two peaks were presented at 150 and 815ºC. The first peak at low temperature may be attributed to the desorption of adsorbed CO_2 on weak basic site, while the second peak may be related to strong basic site of the catalyst. Similar to CH_4 adsorption, it was found that CO_2 adsorption at 750ºC was higher than that at 650ºC. Thus, the activity of this catalyst in carbon dioxide reforming of methane would be better at higher temperatures.

Lastly, N_2 physisorption was also carried out by Micromeritrics model ASAP 2020. The values of BET surface area, pore volume, and pore size of fresh $Ni/SiO_2.MgO$

are 121.43 m^2/g, 0.18 cm^3/g, and 59.52 Å, respectively. The catalyst has pore diameter distribution in mesopore range with the range of 20-100 Å (not shown).

3.2. Catalytic activity in carbon dioxide reforming of methane

The behavior of the carbon dioxide reforming of methane over $Ni/SiO_2.MgO$ catalyst under periodic and steady state operations was investigated at the reaction temperature range of 650-750ºC. For periodic operation, the testing consists of two main steps: (i) methane cracking by feeding methane solely and (ii) regeneration of catalyst via reverse Boudouard reaction by feeding carbon dioxide. In contrast, for steady state operation, the operation was carried out by feeding methane and carbon dioxide simultaneously. It should be noted that the average flow rates of the reactant feeds for both operations were identical. The variations of catalytic reactivities (in terms of methane and carbon dioxide conversions and hydrogen yield) with time at different temperatures under periodic and steady state operations were shown in Figs. 5-6 and Figs. 7-9, respectively.

As shown in Fig. 5 for the periodic operation, at higher temperatures, high methane conversion was achieved at the beginning of reaction but decreased dramatically with reaction time. In contrast, for the periodic testing at lower temperature, methane conversion was almost constant throughout the reaction time. At 750ºC, $Ni/SiO_2.MgO$ catalyst showed high conversion of methane (approximately 67%) at the beginning but declined rapidly to 27% after operating for 240 min, whereas the conversion of methane at reaction temperature 650ºC started at about 48% and remained constant along the reaction time. For the testing at temperatures between 670-730ºC, methane conversions

showed the same trend. The reduction of methane conversion became more pronounced at higher temperatures. Similar trend was observed for carbon dioxide conversion under periodic operation as shown in Fig. 6. It was found that the carbon dioxide conversion at reaction temperature of 750ºC decreased from 55% at the beginning to 24% after 240 min, whereas at reaction temperature of 650ºC, carbon dioxide conversion was nearly constant at 35%. Under the periodic operation, because only the methane cracking takes place during the methane feeding, the hydrogen yield is theoretically equal to the methane conversion. It should be noted that the difference between the methane conversion and carbon dioxide conversion which is particularly large at lower temperature operation indicates that the coke generated during the methane cracking cannot be totally removed and thus accumulated on the catalyst.

Under steady state operation, as shown in Fig. 7, methane conversion did not decrease with increasing reaction time in this range of temperature studied. After exposure for 240 min, the methane conversions at 650, 670, 690, 710, 730, and 750ºC were 63, 73, 83, 81, 84, and 90% respectively. Methane conversions for steady state operation tended to be constant with reaction time and increase with increasing reaction temperature. As shown in Figs. 8-9, carbon dioxide conversions and hydrogen yield tended to be constant with reaction time but did not show clear tendency with reaction temperature. It offered the highest and lowest conversions at reaction temperatures 690 and 710ºC respectively. This is probably affected by the occurrence of the reverse water-gas shift reaction.

Comparison of the catalyst activity under the periodic operation with the steady state operation in this range of reaction temperature revealed that Ni/SiO_2.MgO showed

stability under the steady state operation. In contrast, under the periodic operation, the catalyst showed stability at low temperature but showed a rapid decline of activity over reaction time at high temperature. The reason for catalyst deactivation was then further investigated. Theoretically, the deactivation should be mainly due to the formation of carbon species on the surface of catalyst. It was suggested that, at different operating temperatures, various types of coke formation could occur on the surface of catalyst and affect the catalytic activity under periodic operation. Thus, characterization of spent catalyst was carried out to clarify the catalyst testing results, as presented in the next section.

3.3. Characterization of spent catalysts

Firstly, the changes in weight of catalyst were considered to be related to the degree of coke formation on the surface of spent catalysts. Fig. 10 shows the weights of catalyst at various reaction times and temperatures. It is clear that both reaction temperature and reaction time influence the change in catalyst weight. According to this figure, at the beginning, the catalyst was reduced with hydrogen to form metallic phase of nickel species, the weight of reduced catalyst decreased about 5.5%. Then the reforming reaction under periodic operation started and the weights of used catalysts were measured at reaction time of 90 min which was ending time of a methane cracking period. It was found that lower coke formation was observed in the system at higher reaction temperature. At the reaction time of 100 min which was ending time of a regeneration period, it was found that significant amount of coke could not be removed and remained present in the system at lower reaction temperature. Similar trends were observed at

reaction times of 190 and 200 min. It is interesting that the methane conversion still remained high for low temperature operation although the significant increase of coke accumulation was observed. This phenomenon was possibly affected by the forming of various types of coke at different reaction temperatures.

Table 1 presents the BET studies over catalyst at different conditions. It was found that reaction temperature and reaction time also affected the surface area of catalyst. The BET surface area of fresh catalyst is 104.62 m^2/g. Reducing the catalyst at 650°C with hydrogen decreased the BET surface area to 46.96 m^2/g due to the surface sintering and the change of NiO to metallic nickel. In order to investigate the effect of sintering on BET surface area, the fresh catalyst was also calcined in air at 750ºC for 3 h. It was found that high temperature dramatically affected on BET surface area of the catalyst. It should be noted that the amount of coke formed also affects the specific surface area of catalyst; at low temperature under periodic operation, BET surface areas increased after methane cracking period and decreased after regeneration with carbon dioxide.

TPO testing of used catalysts at different reaction times and reaction temperatures were carried out (Figs. 11(a)-(f)). The principle of TPO is to evaluate the amount of coke removed from the used catalyst by burning with oxygen. According to the results, the profile revealed two peaks of coke at oxidizing temperatures ca. 530 and 880ºC. The first peak was narrow and high whereas the second peak was board and low. This strongly indicates that at least 2 different types cokes were formed on the surface of catalyst. It should also be noted that after the regeneration by carbon dioxide the first peak at low

temperature shifted to a higher temperature, indicating that some easily combusted coke was removed from the catalyst surface.

The SEM micrographs of used catalysts from periodic operation in the range of reaction temperature between 650-750ºC are shown in Figs. 12(a)-11(f). The SEM experiments were carried out using JEOL JSM-35F scanning electron microscope operated under the back scattering electron (BSE) mode at 20 kV. All samples were tested after exposure in the reaction for 190 min, which was the ending time of methane cracking period. It can be seen that carbon formation in carbon dioxide reforming of methane presented the structure of filamentous carbon on the surface of catalyst over this range of temperature. From the literature, it was found that the formation of this type of carbon induced a serious pressure drop in the reactor [11]. Other type of carbon which was expected to form over this range of temperature is the encapsulated carbon. It was believed that the encapsulated carbon strongly affects the stability of catalyst by blocking the active site of metallic catalyst, nevertheless, it is difficult to prove the formation of encapsulated carbon by SEM micrograph. From SEM results, filamentous carbon was obviously found on the surface of catalyst for all reaction temperatures. It was also observed that when the high temperature was employed, the larger particle size of filamentous coke was observed.

The crystallinity and structure of catalysts were analyzed by XRD analysis. The XRD analysis was performed by a SIEMENS D5000 X-ray diffractometer connected with a personal computer with Diffract AT version 3.3. The measurement was carried out by using CuK_{α} radiation with Ni filter. The step-scan covered the angular range 10-80° (2θ) in steps of 2θ = 0.04°. The XRD patterns of used catalysts at reaction temperature

range of 650-750ºC are shown in Figs. 13(a)-(f). These patterns presented evidently the strong peaks at 2θ = 26.6 and 44.5º and several low intensity peaks at certain degrees for all samples. The peak at 2θ = 26.6º was attributed to be the coke deposited on the surface of the catalyst. The presence of main structure of metallic Ni showed peaks at 2θ = 44.5, 51.8, and 76.4º. The crystal structure of NiO was also observed for low intensity peaks at 2θ = 37.1, 43.1 and 62.7º. For tendency, higher and sharper intensity peaks of coke and Ni were found when reaction temperature was higher. This XRD results indicated that there were the differences of catalyst particle sizes at various reaction temperatures. The d-spacing of nickel and coke were then calculated by Scherrer equation as shown in Table 2. The d-spacing of nickel was obtained from peak at 44.5º whereas that of coke was obtained from peak at 26.6º. It was found that when the higher temperature was used, the higher d-spacing for both nickel and coke were obtained; this is mainly due to the effect of catalyst sintering. This result was corresponding to the result of BET surface area as high value of d-spacing induced size of particle to be larger and lessened BET surface area. It should also be noted that the d-spacing increased after regeneration with carbon dioxide and decreased after methane cracking in the next cycle. High values of d-spacing for both nickel and coke caused the blockage of active site of catalyst. Thus, it was probable to bring to the loss of stability of catalyst.

From the above results it is likely that the at low temperature under periodic operation, greater amount of coke was formed as filamentous carbon during the methane cracking period and was incompletely removed during the regeneration period. However, the deposition of this type of coke did not significantly affect the activity of catalyst. In contrast, at high temperature, lesser amount of coke was obtained but in the form of

encapsulating carbon which strongly affected the activity of catalyst and resulted in the rapid catalyst deactivation.

4. Conclusion

The carbon dioxide reforming of methane under the periodic and steady state operations in a range of reaction temperature between 650-750^{o}C was compared. It was found that Ni/SiO_2.MgO catalyst showed good stability under steady state operation for all operating temperatures, but showed stability only at low temperature for the periodic operation. According to the spent catalyst characterizations, carbon formation from carbon dioxide reforming of methane under periodic operation at the reaction temperature range 650-750^{o}C presented at least two different types of coke taking place on the surface of catalyst. At low temperature, great amount of coke was formed during the methane cracking period and was incompletely removed during the regeneration period. At this temperature, coke was mostly formed in the structure of filamentous carbon. In contrast, at high temperature, a lesser amount of coke was obtained but it was formed in encapsulating form which strongly affected the activity of catalyst and resulted in the rapid catalyst deactivation.

Acknowledgement

The research was financially supported by the Thailand Research Fund, Commission on Higher Education and the Graduate School of Chulalongkorn University. The authors also would like to thank Professor Goto and Professor Tagawa for providing the catalyst.

References

[1] B. Monnerat, L. Kiwi-Minsker, and A. Renken, Chem. Eng. Sci., 56, (2001), 633.

[2] T. Sodesawa, A. Dobashi and F. Nozaki, React. Kinet. Catal. Lett., 12, (1979), 107.

[3] L. Topor, L. Bejan, E. Ivana, N. Georgescu, Revue Chim. Bucharest, 30, (1979), 539.

[4] T.A. Chubb, Sol. Energy, 24, (1980), 341.

[5] T.A. Chubb, J.H. McCrary, G.E. McCrary, J.J. Nemecek and D.E. Simmons, Proc. Meet. Am. Sect. Int. Sol. Eng. Soc., 4, (1981), 166.

[6] J.R. Rostrup-Nielsen and J.H. Bak Hansen, J. Catalysis, 144, (1993), 38.

[7] A. Erdöhelyi, J. Cserényi and F. Solymosi., J. Catal., 141, (1993), 287.

[8] A. Erdöhelyi, J. Cserényi, E. Rapp and F. Solymosi., Appl. Catal. A: Gen., 108, (1994), 205.

[9] J. Nakamura, K. Aikawa, K. Sato and T. Uchijima., Catal. Lett., 25, (1994), 265.

[10] Z.L. Zhang, V.A. Tsipouriari, A.M. Efstathiou and X.E. Verykios., J. Catal., 158, (1996), 51.

[11] Takano, A., Tagawa, T., and Goto, S. Journal of Chemical Engineering of Japan, 27, (1994), 727.

Figure

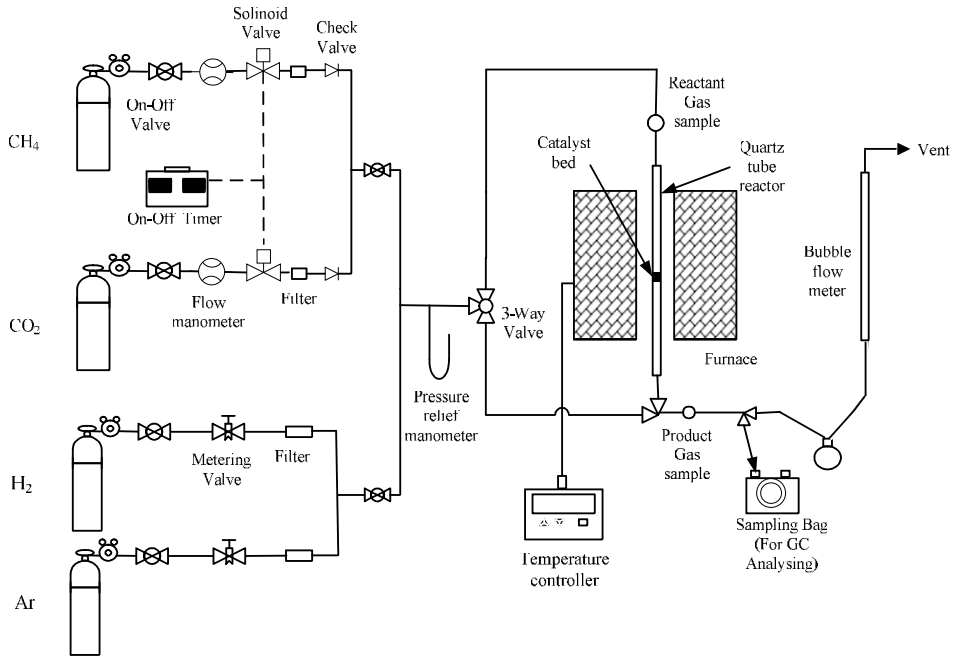

Fig.1 - Schematic diagram of the experimental setup.

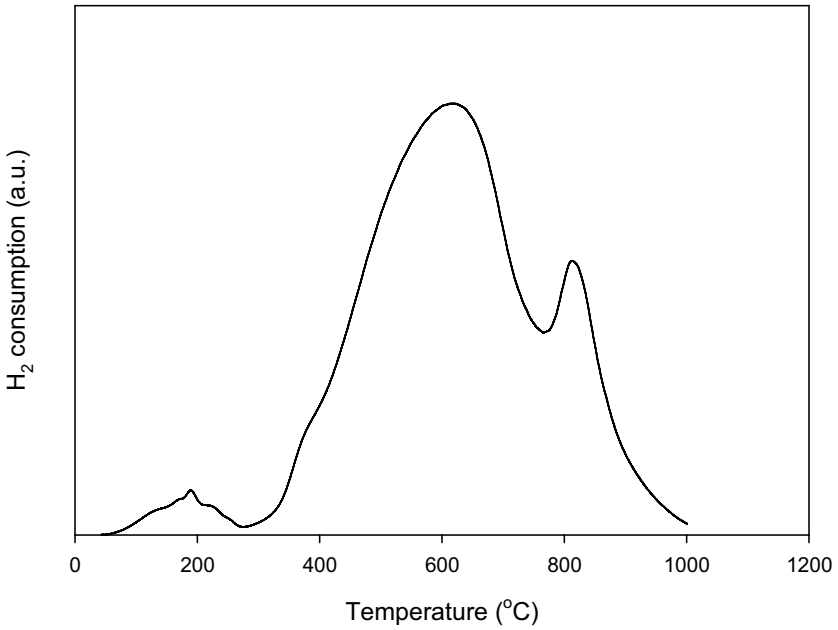

Fig. 2 - Temperature-programmed reduction profile of fresh catalyst.

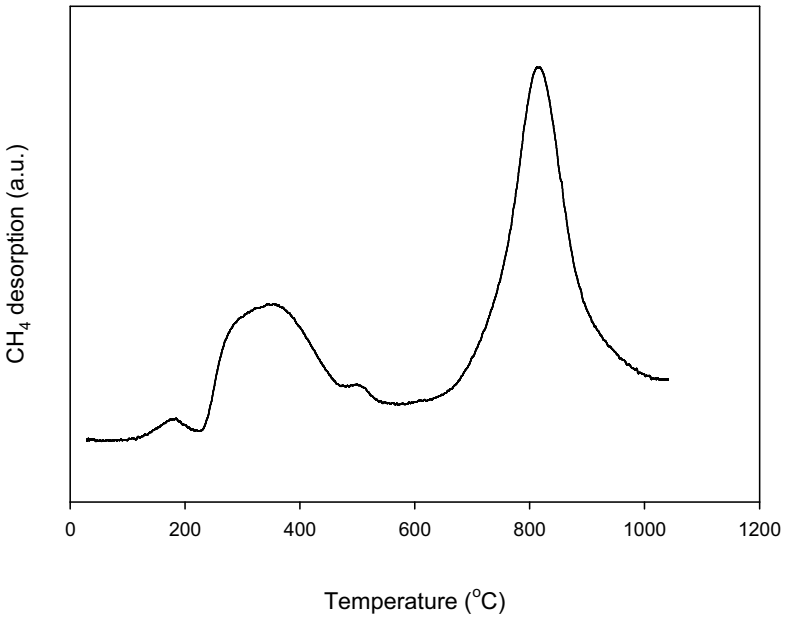

Fig. 3 - CH_4 temperature-programmed desorption profile of fresh catalyst.

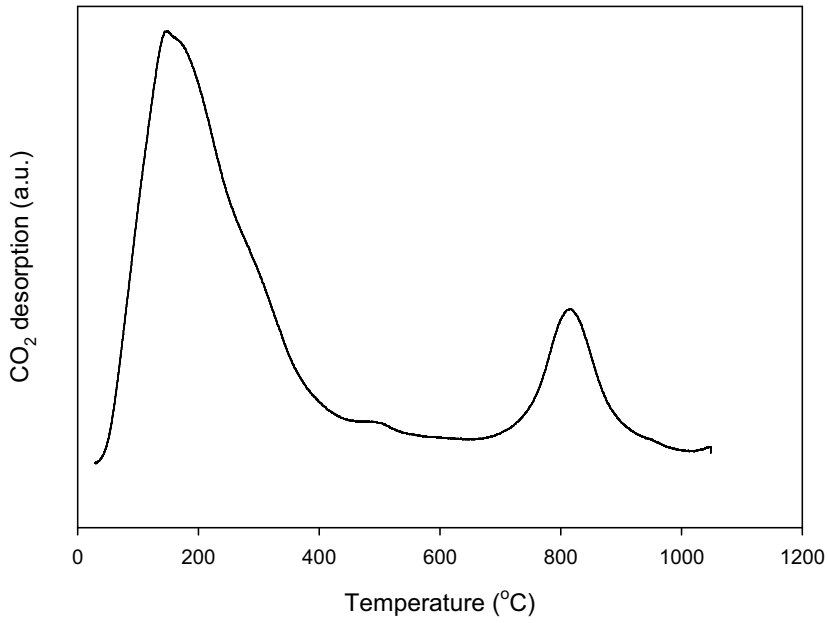

Fig. 4 - CO_2 temperature-programmed desorption profile of fresh catalyst.

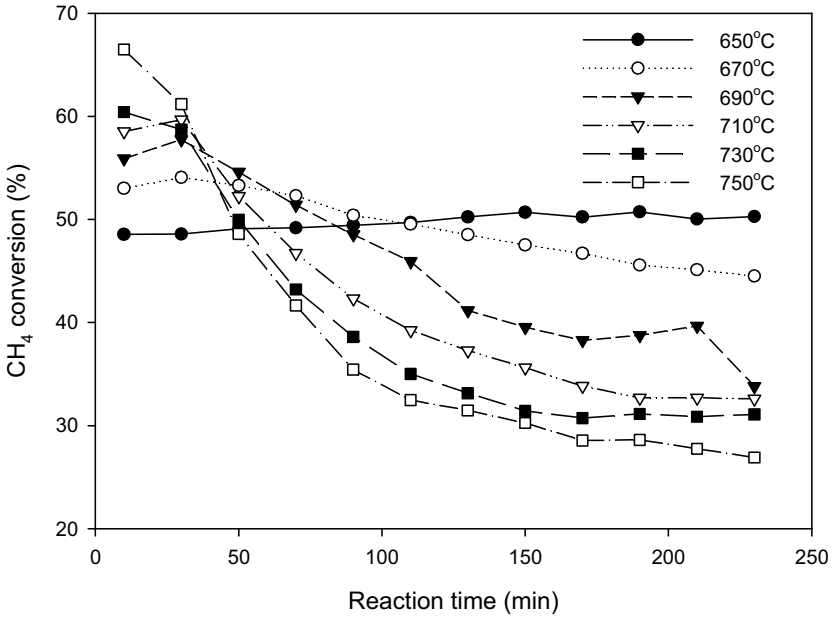

Fig. 5 - Methane conversion in carbon dioxide reforming of methane reaction under periodic operation at different reaction temperatures.

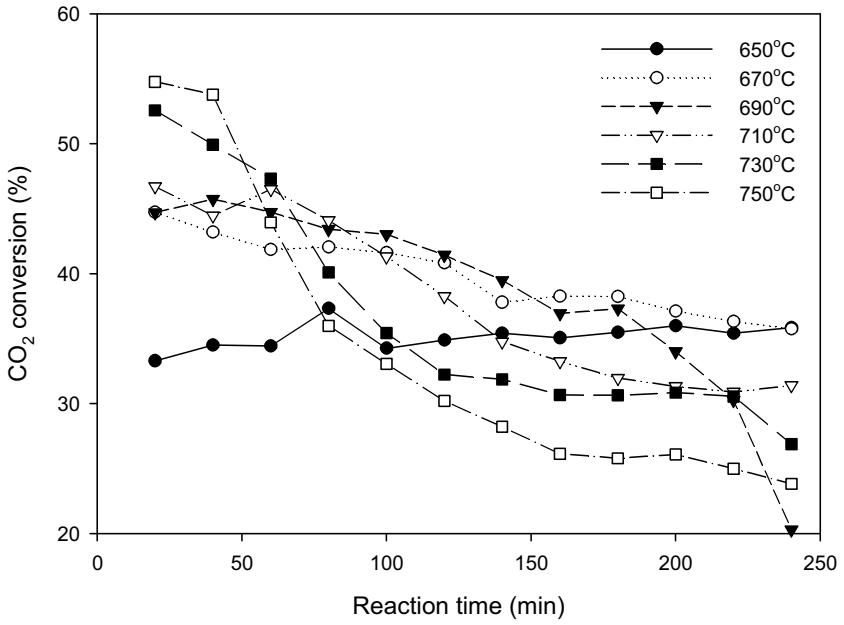

Fig. 6 - Carbon dioxide conversion in carbon dioxide reforming of methane reaction under periodic operation at different reaction temperatures.

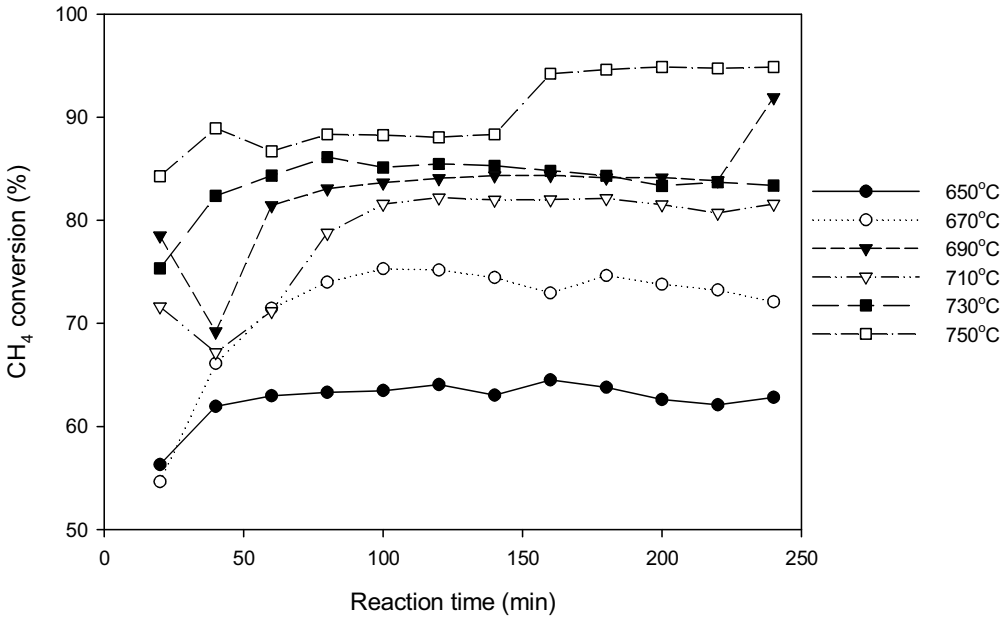

Fig. 7 - Methane conversion in carbon dioxide reforming of methane reaction under steady state operation at different reaction temperatures.

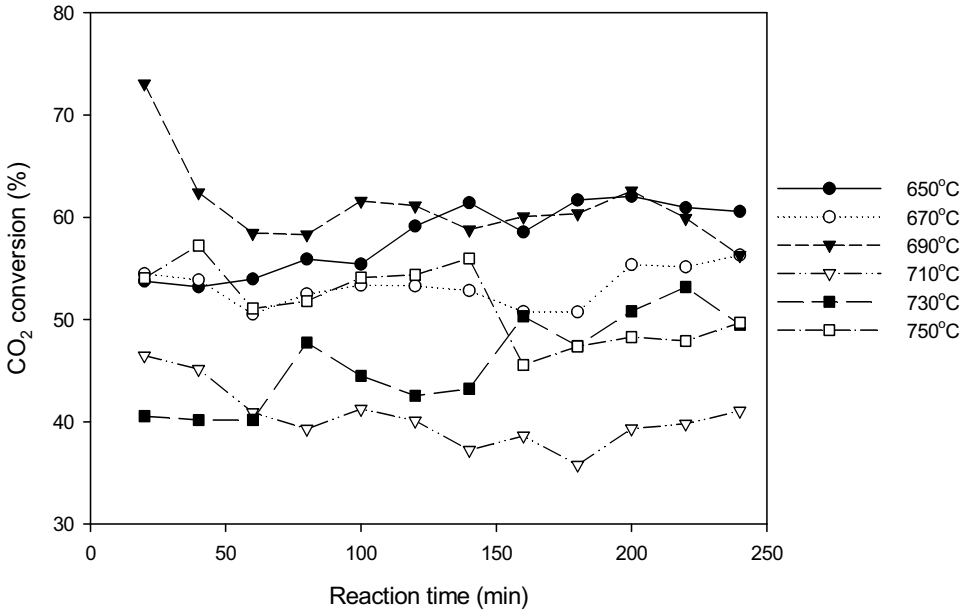

Fig. 8 - Carbon dioxide conversion in carbon dioxide reforming of methane reaction under steady state operation at different reaction temperatures.

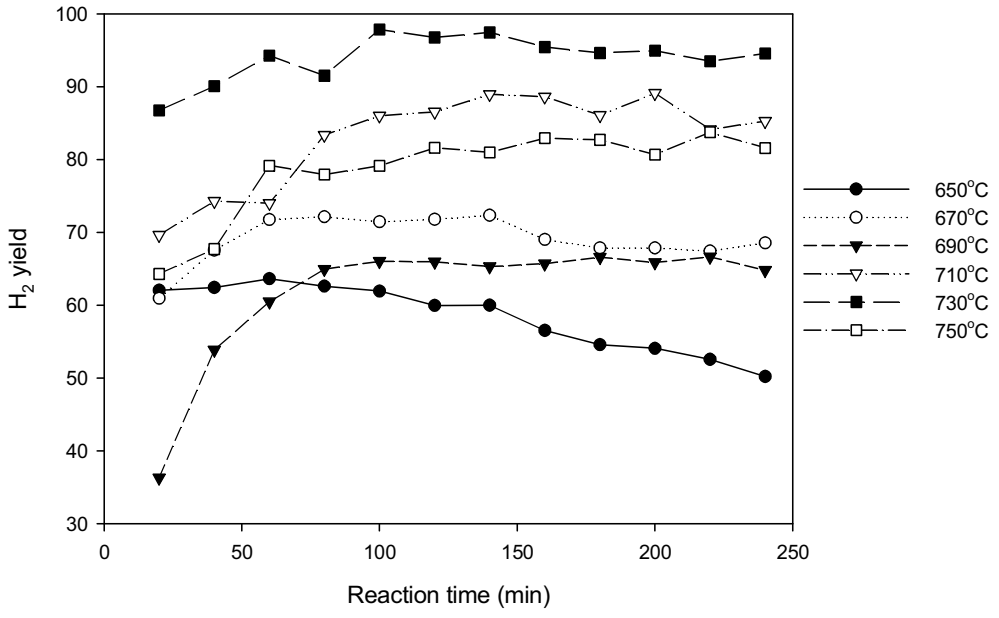

Fig. 9 - Hydrogen yield in carbon dioxide reforming of methane reaction under steady state operation at different reaction temperatures.

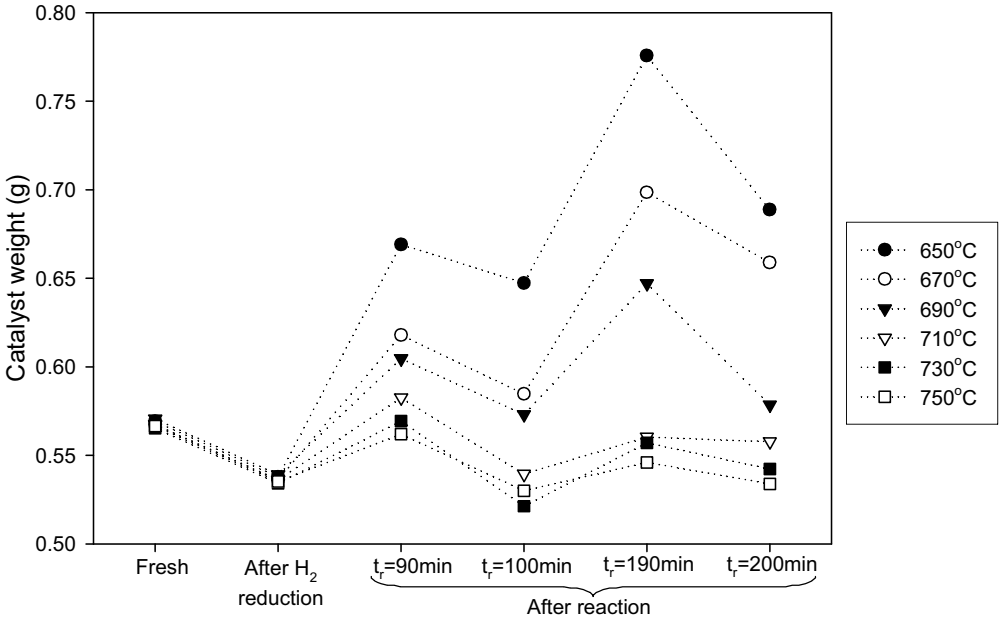

Fig. 10 - Catalyst weights before and after reaction.

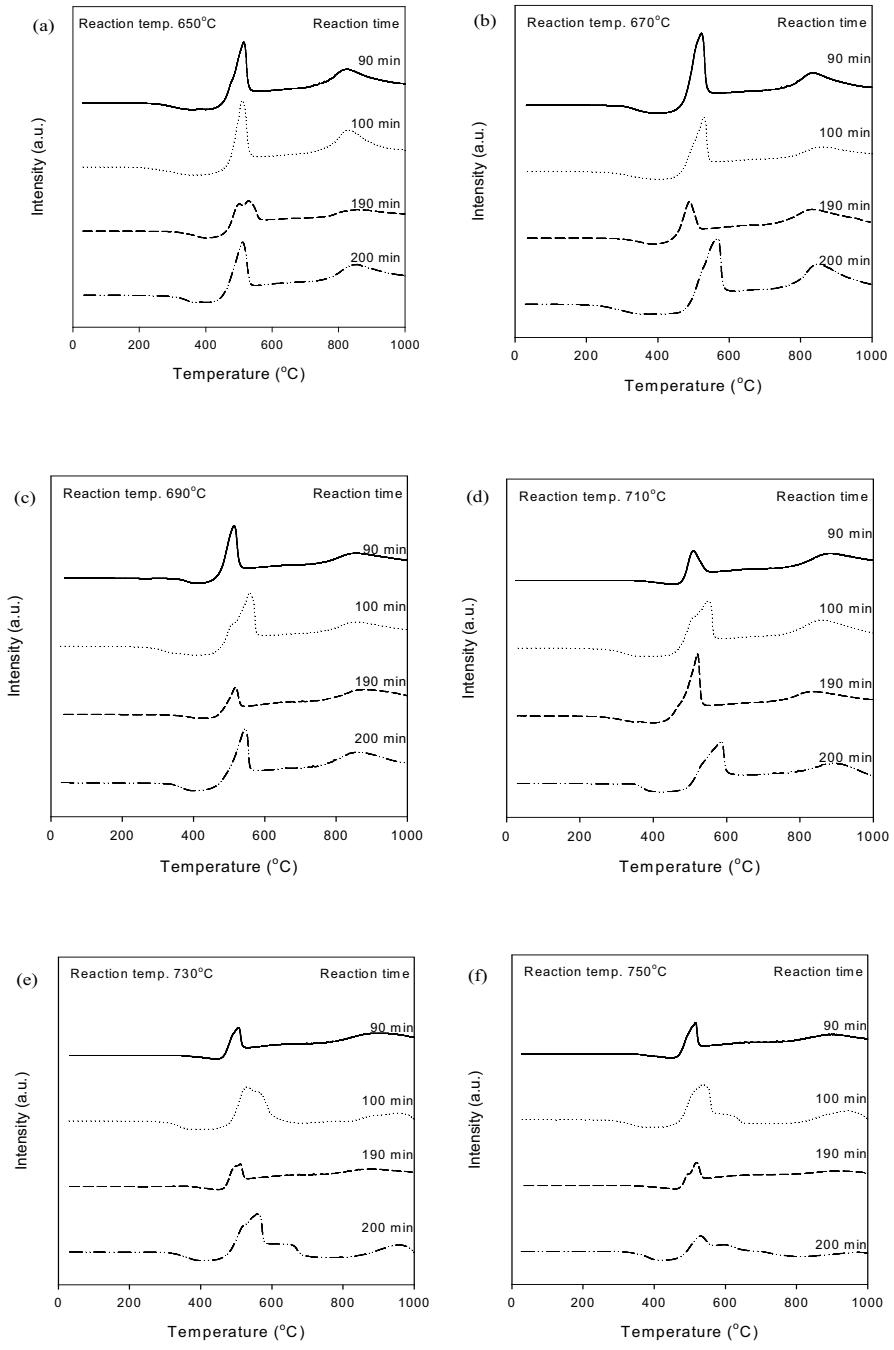

Fig. 11 - TPO profiles of used catalysts at different reaction times and reaction temperatures (a) at 650ºC (b) at 670ºC (c) at 690ºC (d) at 710ºC (e) at 730ºC and (f) at 750ºC.

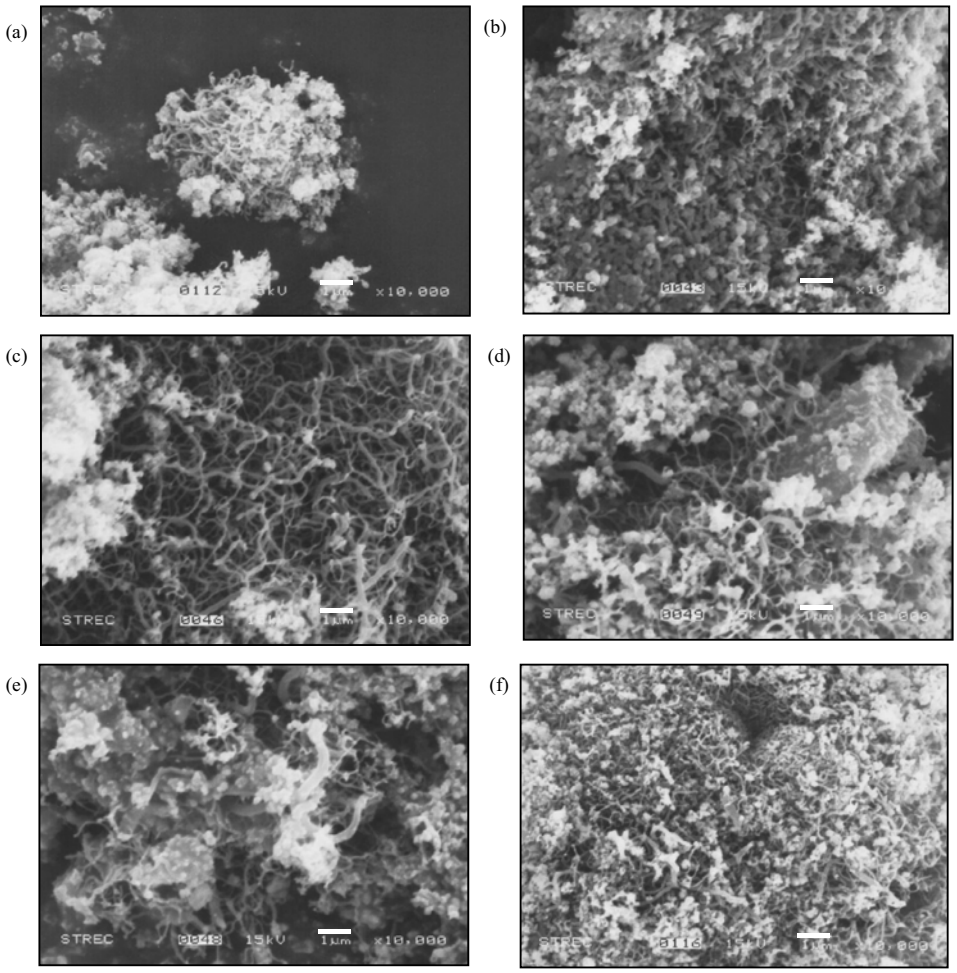

Fig. 12 - SEM micrographs of used catalysts at reaction time = 190 minutes and different reaction temperatures: (a) at 650ºC (b) at 670ºC (c) at 690ºC (d) at 710ºC (e) at 730ºC and (f) at 750ºC.

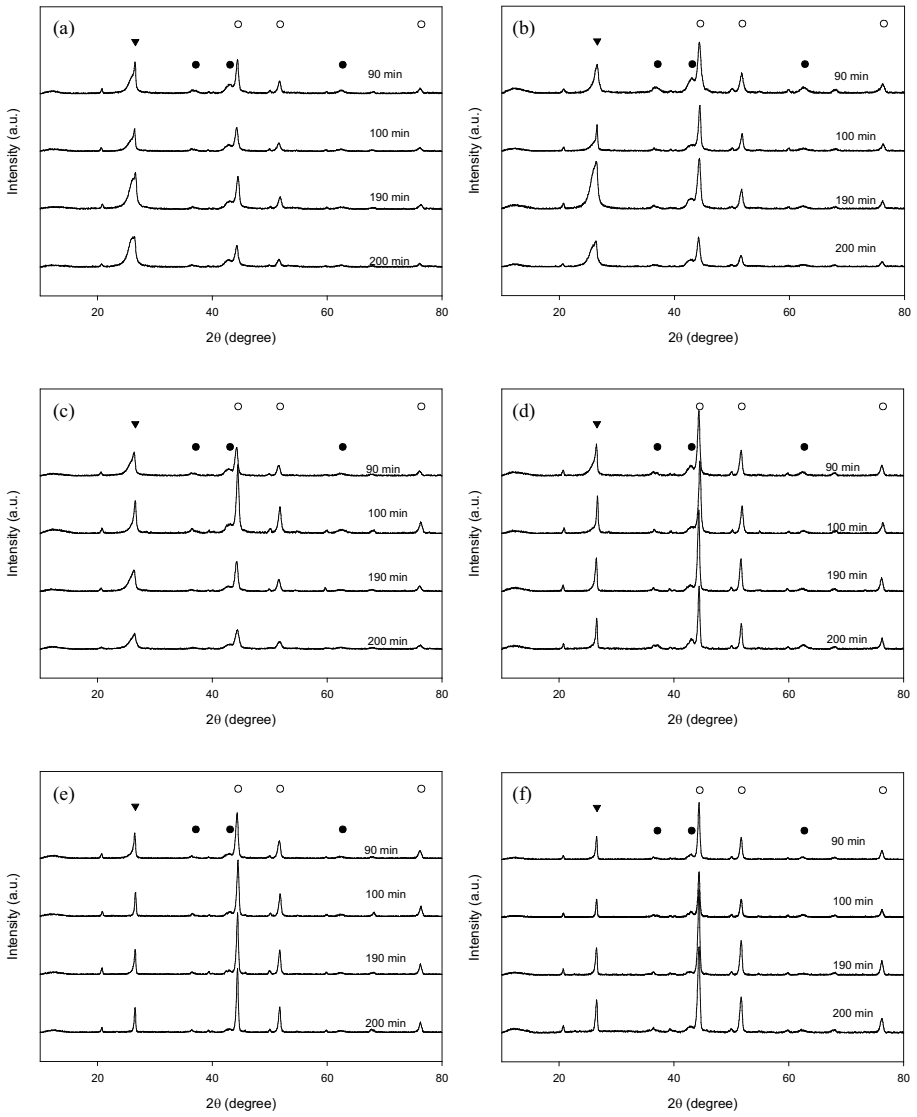

Fig. 13 - XRD patterns of used catalysts at different reaction times and reaction temperatures (a) at 650ºC (b) at 670ºC (c) at 690ºC (d) at 710ºC (e) at 730ºC and (f) at 750ºC ▾ Coke ◦ Ni • NiO.

Table 1 - BET surface areas of catalysts at different conditions.

Catalysts	Surface area (m^2/g)			
Fresh	104.62			
After reduction with hydrogen at 650ºC	46.96			
After calcination in air at 750ºC 3 h	45.43			
After reaction at	reaction time			
reaction temperature	90 min	100 min	190 min	200 min
650ºC	56.24	60.51	76.56	64.99
670ºC	33.94	50.11	78.24	51.69
690ºC	47.77	33.56	65.52	59.07
710ºC	47.89	35.95	32.30	18.55
730ºC	31.24	20.97	17.94	14.54
750ºC	20.74	19.36	20.42	14.06

Table 2 - The d-spacing of nickel and coke deposited on catalysts at different conditions.

Catalysts	d-spacing of nickel (nm)				d-spacing of coke (nm)			
Fresh	4.83				-			
After reaction at	reaction time							
Reaction temperature	90 min	100 min	190 min	200 min	90 min	100 min	190 min	200 min
650ºC	18.23	14.96	14.90	13.86	9.82	10.09	6.50	5.73
670ºC	12.97	22.72	14.54	15.45	10.39	29.26	6.34	5.95
690ºC	15.60	19.32	15.04	11.16	8.38	17.66	7.03	7.62
710ºC	20.80	22.69	25.96	27.61	16.44	33.40	24.52	31.04
730ºC	19.53	26.23	29.25	30.69	23.88	37.79	30.03	39.48
750ºC	26.88	28.25	27.92	20.90	35.75	39.34	27.36	26.10